

**COMPARATIVE STUDY OF DIFFERENT TRANSFORMS
IN OFDM COMMUNICATION SYSTEM**

A DISSERTATION

**SUBMITTED IN PARTIAL FULFILLMENT OF THE REQUIREMENTS
FOR THE AWARD OF THE DEGREE
OF**

**MASTER OF TECHNOLOGY
IN
MICROWAVE AND OPTICAL COMMUNICATION**

Submitted by:

**SIDDHANT JAIN
2K14/MOC/18**

Under the supervision of

DR. PRIYANKA JAIN



**DEPARTMENT OF ELECTRONICS AND
COMMUNICATION AND APPLIED PHYSICS**

DELHI TECHNOLOGICAL UNIVERSITY

(Formerly Delhi College of Engineering)

Bawana Road, Delhi-110042

JUNE, 2019

**DEPARTMENT OF ELECTRONICS &
COMMUNICATION ENGINEERING AND APPLIED
PHYSICS**

DELHI TECHNOLOGICAL UNIVERSITY

(Formerly Delhi College of Engineering)

Bawana Road, Delhi-110042

CANDIDATE'S DECLARATION

I Siddhant Jain, Roll No. 2K14/MOC/18 student of M.Tech (Microwave and Optical Communication), hereby declare that the project Dissertation titled “Comparative Study of Different Transforms in OFDM communication system” which is submitted by me to the Department of Electronics and Communication Engineering and Applied Physics, Delhi Technological University, Delhi in partial fulfillment of the requirement for the award of the degree of Master of Technology, is original and not copied from any source without proper citation. This work has not previously formed the basis for the award of any Degree, Diploma, and Associateship, Fellowship or other similar title or recognition.

Place: Delhi

(SIDDHANT JAIN)

Date:

**DEPARTMENT OF ELECTRONICS &
COMMUNICATION ENGINEERING AND APPLIED
PHYSICS**

DELHI TECHNOLOGICAL UNIVERSITY

(Formerly Delhi College of Engineering)

Bawana Road, Delhi-110042

CERTIFICATE

I hereby certify that the Project Dissertation titled “Comparative Study of Different Transforms in OFDM communication system” which is submitted by Siddhant Jain, Roll No 2K14/MOC/18 [Department of Electronics and Communication Engineering and Applied Physics], Delhi Technological University, Delhi in partial fulfillment of the requirement for the award of the degree of Master of Technology, is a record of the project work carried out by the student under my supervision. To the best of my knowledge this work has not been submitted in part or full for any Degree or Diploma to this University or elsewhere.

Place: Delhi

DR. PRIYANKA JAIN

Date:

SUPERVISOR

ASSISTANT PROFESSOR

ABSTRACT

The topic of the project is ‘Comparative Study of Different Transforms in OFDM communication system’. Over the year’s communication systems have evolved with a rapid pace. The need for ultra fast, ultra reliable and service in any scenario has resulted in better communication systems over the years. The current standard of 4G uses OFDM which effectively transforms a wideband frequency selective channel into a band of parallel flat-fading channels. This is a multi-carrier scheme which is made possible by the use of DFT and IDFT operation. However, there are problems of Carrier-Frequency Offset and high PAPR in OFDM. Also the DFT and IDFT use complex computations.

The problem of high PAPR can be reduced using SC-FDMA. Using MATLAB conventional OFDM systems has been simulated for different digital modulation schemes for AWGN channel and BER has been plotted. Also the SC-FDMA system has been simulated and PAPR has been compared with conventional OFDM. Also both the conventional and SC-FDMA systems have been simulated using DCT and DST and BER and PAPR analysis has been done. These transforms use real coefficients only and thus, can be effectively used instead of DFT as DFT involves complex computations.

ACKNOWLEDGEMENT

Humans are curious by nature and curiosity leads to research. To satisfy the thirst for knowledge, people go on enquiring more and more facts. But without the help and co-operation of other individuals, it is not possible for them to reach at any conclusion. I consider myself extremely fortunate that I had an opportunity of doing my project under invaluable guidance of my mentor **Dr. Priyanka Jain**. I would like to thank her for her precious suggestions, support and technical help during the course of this project.

I am also grateful to those who have directly or indirectly helped during the course of the project. And lastly I am grateful to my family for supporting me in completing this project.

SIDDHANT JAIN

CONTENTS

Declaration	i
Certificate	ii
Acknowledgment	iii
Abstract	iv
Contents	v
List of Tables	viii
List of Figures	ix
List of Abbreviations	xi
Chapter 1- INTRODUCTION	1-4
1.1 Motivation	2
1.2 Literature Survey	3
1.3 Thesis Organization	4
Chapter 2- OFDM: A MULTI-CARRIER MODULATION SYSTEM	5-13
2.1 Introduction to OFDM	5
2.2 Drawbacks of OFDM	11
2.2.1 Effect of frequency offset	11
2.2.2 High PAPR	13
Chapter 3- DFT-s-OFDM	14-19
3.1 Introduction to SC-FDMA	14
3.2 Introduction to DFT-s-OFDM	15

3.3	Time domain representation of different spreading techniques	17
3.3.1	Time Domain representation of IFDMA	16
3.3.2	Time Domain representation of DFDMA	18
3.3.3	Time Domain representation of LFDMA	18
Chapter 4- TRANSFORMS		20-23
4.1	Introduction to transforms	20
4.2	Discrete Fourier Transform (DFT)	20
4.3	Discrete Cosine Transform (DCT)	22
4.4	Discrete Sine Transform (DST)	23
Chapter 5- SIMULATION RESULTS		24-46
5.1	Simulation model for OFDM over AWGN channel	24
5.1.1	BER for QPSK	25
5.1.2	BER for 16-QAM	26
5.1.3	BER for 64-QAM	26
5.1.4	BER comparison for OFDM in AWGN channel	27
5.2	Simulation model for DFT-s-OFDM over AWGN channel	28
5.3	Simulation results for LFDMA	29
5.3.1	BER for case of $M = 64$	29
5.3.2	BER for case of $M = 128$	30
5.4	Simulation results for DCT and DST spreading	37
5.4.1	Simulation results for IFDMA	37

5.4.2	Simulation results for DFDMA	38
5.4.3	Simulation results for LFDMA	39
5.5	Simulations for PAPR analysis	40
5.5.1	PAPR performance for QPSK	41
5.5.2	PAPR performance for 16-QAM	42
5.5.3	PAPR performance for 64-QAM	43
5.5.4	PAPR performance for different transforms for IFDMA	44
5.5.5	PAPR performance for different transforms for DFDMA	45
5.5.6	PAPR performance for different transforms for IFDMA	46
Chapter 6- CONCLUSION AND FUTURE WORK		47
Appendix 1- MATLAB CODE FOR BER AND PAPR SIMULATION		48-59
REFERENCES		60-61

LIST OF TABLES

Table 3.1: IFFT block output for different spreading algorithms	19
Table 4.1: Properties of DFT	21
Table 5.1: Simulation parameters for OFDM system	24
Table 5.2: BER v/s SNR values for QPSK	25
Table 5.2: BER v/s SNR values for 16-QAM	26
Table 5.4: BER v/s SNR values for 64-QAM	26
Table 5.5: Simulation parameters for DFT-s-OFDM	28
Table 5.6: BER values for LFDMA with $M = 64$	29
Table 5.7: BER values for LFDMA with $M = 128$	31

LIST OF FIGURES

Fig. 2.1 : Multi-Carrier Modulation System	5
Fig. 2.2 : Comparison of symbol duration for MC and SC systems	6
Fig. 2.3 : Block diagram of OFDM system	7
Fig. 2.4 : OFDM symbol without Cyclic-Prefix	8
Fig. 2.5 : Addition of Cyclic-Prefix	8
Fig. 2.6 : Effect of adding Cyclic-Prefix	9
Fig. 2.7 : Block diagram of CP-OFDM system	10
Fig. 2.8 : Effect of Carrier Frequency Offset	11
Fig. 3.1 : Block diagram of DFT-s-OFDM system	14
Fig. 3.2 : IFDMA mapping	15
Fig. 3.3 : DFDMA mapping	15
Fig. 3.4 : LFDMA mapping	16
Fig. 5.1: OFDM simulation model	24
Fig. 5.2 : BER comparison for different modulation schemes	27
Fig. 5.3 : Simulation model for DFT-s-OFDM	28
Fig. 5.4 : BER comparison for LFDMA with $M = 64$	30
Fig. 5.5 : BER comparison for LFDMA with $M = 128$	31
Fig. 5.6 : BER comparison of LFDMA and OFDM for QPSK	32
Fig. 5.7 : BER comparison of LFDMA and OFDM for 16-QAM	33
Fig. 5.8 : BER comparison of LFDMA and OFDM for 64-QAM	34
Fig. 5.9 : BER comparison of different spreading technique($M = 64$)	35
Fig. 5.10 : BER comparison for $M = 128$	36
Fig. 5.11 : BER comparison for IFDMA	37
Fig. 5.12 : BER comparison for DFDMA	38
Fig. 5.13 : BER comparison for LFDMA	39
Fig. 5.14: Effect of N on PAPR	40
Fig. 5.15 : PAPR performance in QPSK	41
Fig. 5.16 : PAPR performance in 16-QAM	42

Fig. 5.17 : PAPR performance in 64-QAM	43
Fig. 5.18: PAPR performance of different transforms in LFDMA	44
Fig. 5.19: PAPR performance of different transforms in DFDMA	45
Fig. 5.20: PAPR performance of different transforms in IFDMA	46

LIST OF ABBREVIATIONS

BER	Bit Error Rate
BPSK	Binary Phase Shift Key
CDMA	Code Division Multiple Access
CFO	Carrier Frequency Offset
DCT	Discrete Cosine Transform
DFDMA	Distributed Frequency Division Multiple Access
DFT	Discrete Fourier Transform
DFT-s-	
OFDM	Discrete Fourier Transform Spread OFDM
DST	Discrete Sine Transform
FDMA	Frequency Division Multiple Access
FFT	Fast Fourier Transform
ICI	Inter-Channel Interference
IDCT	Inverse Discrete Cosine Transform
IDFT	Inverse Discrete Fourier Transform
IDST	Inverse Discrete Sine Transform
IFDMA	Interleaved Frequency Division Multiple Access
IFFT	Inverse Fast Fourier Transform
IMT	International Mobile Telecommunications
ISI	Inter-Symbol Interference
LFDMA	Localized Frequency Division Multiple Access
OFDM	Orthogonal Frequency Division Multiplexing
PAPR	Peak to Average Power Ratio
QAM	Quadrature Amplitude Modulation
QPSK	Quadrature Phase Shift Key
SC-FDMA	Single Carrier- Frequency Division Multiple Access
TDMA	Time Division Multiple Access

CHAPTER 1

INTRODUCTION

A basic communication system helps in reliable exchange of information between a source or transmitter and destination or receiver through a channel such as air, deep space or optical fiber. The word reliable is important as the channel corrupts the information sent over the channel. This corruption of information or introduction of noise often leads to erroneous decoding at the destination and loss of data.

A digital communication system consists of a transmitter, channel and receiver. Any useful data at the transmitter is converted into a signal which can be passed over the channel. This conversion of useful data into a signal is called modulation and the signal is then demodulated at the receiver and put to further use. Usually the data is modulated onto a single carrier and thus, the whole bandwidth is used by each symbol. But as data rates become higher the required bandwidth increases. This leads to problems when the channel is frequency selective. In a frequency selective channel when the bandwidth is greater than the coherence bandwidth symbols experience Inter-Symbol-Interference (ISI).

This problem can be mitigated by using Multi-Carrier (MC) systems. These systems use different frequencies or multiple frequencies for transmission for each symbol. The bandwidth is divided such that the bandwidth of each carrier is less than the coherence bandwidth. Thus, by dividing the available bandwidth into several narrowband sub-channels the frequency selective channels perceives each band of frequency as 'flat'. Orthogonal Frequency Division Multiplexing (OFDM) is one such MC system where the sub-carriers are orthogonal to each other. OFDM scheme is able to provide for large data rates and is robust to radio channel impairments.

1.1 MOTIVATION

Over the years the need for sending more and more data to everyone and at a faster rate and without any delay has resulted in evolution of communication systems. In 1970, the first generation communication system (designated as 1G) was able to transmit just analog voice over wires using the technique of FDMA. By 1990s the second generation system (or 2G) had developed and it was possible to transmit digital signals over air. This was popularly known GSM and used the technique of TDMA and CDMA. The data rates achieved were in the range of 9.6 to 28.8 Kbps. The modulation schemes used in this were GMSK and 8-PSK

The next stage of evolution was 2.5G commonly known as EDGE and GPRS which had data rates of 57 to 115 Kbps. The 3G systems used WCDMA and data rates further increased to 0.144 to 2 Mbps. This had voice and non-voice signals for ‘mobile’ users and used QAM for modulation. By 2007, 3.5G systems like HSPA and WiMAX had developed and achieved data rates of 10’s of Mbps. By 2010 4G systems (also known as IMT-A) had been deployed which used the technique of OFDMA. Current communication systems are 4G systems with data rates in the range of 100’s of Mbps.

The process of evolution has not only increased the data rates (from Kbps in 1G to Mbps in 3G and 4G), but has also improved the quality of service. The FDMA scheme was bad at utilizing the spectrum efficiently. TDMA scheme performance was limited by problem of multi-path fading. Also there problems like call – drops, cross-connection, bad signals in rural areas etc. These problems have reduced over generation of communication systems. Thus, one of the goals of this process of evolution has also been to provide better service to everyone and everywhere. This process of evolution has not stopped and will continue forever as demand for faster data rates and ultra-reliable communication with low-latency increases.

The future generations have always tried to improve upon the previous generations and have been made possible by improving the existing technologies. This is also true for the future generation or 5G (called 5G NR). The main requirements for 5G (also called IMT-2020) are faster efficient and intelligent system. The recent research for waveforms for 5G have thus focused attention on improving the waveform used for 4G i.e. OFDM.

1.2 LITERATURE SURVEY

The concept of Frequency Division Multiplexing (FDM) was introduced in mid 60's [1, 2] for parallel data transmission. The frequency band was divided into smaller bands which were allocated to different users. This concept has evolved into OFDM 4G systems in which orthogonal sub-carriers are used and is a multi-carrier (MC) scheme. In general Multi-Carrier Modulation Systems were difficult to design as it involved designing a bank of modulators and demodulators. OFDM was made possible by work of Weinstein and Ebert [3]. They were able to apply the DFT [4] to parallel data transmission system for modulation and demodulation process.

OFDM has been adopted as standard in Digital Video Broadcast (DVB) and Digital Audio Broadcast (DAB). OFDM is a standard in indoor wireless systems such as IEEE 802.11 and hiperlan2 [5]. OFDM has found use in high speed modems and digital mobile communications. Recently OFDM was exploited for wideband data communications over mobile radio FM channels, wireless LAN wireless multimedia communication, and many other applications [6]

The conventional OFDM system has a cyclic prefix to combat the problem of ISI in multipath channel. Other alternatives have been proposed like Zero-Padding (ZP) [7]. In [8-10] the use of Unique Word (UW) has been proposed where instead of cyclic-prefix known sequences are used as guard band for ISI reduction. A Zero-tail DFT-spread-OFDM signal has been proposed in [11, 12] where instead of a cyclic prefix zeros are added in the head and tail of OFDM symbol to combat the effect of ISI channel.

OFDM requires precise carrier synchronization and has high PAPR problem. SC-FDMA is alternative for reducing the PAPR but it still requires synchronization. It has been adopted as the uplink access scheme in LTE (Long Term Evolution). Many different variations of OFDM have been proposed for 5G. A scheme proposed the use of filters or F-OFDM [13] to reduce the effect of CFO. Another paper has proposed Generalized OFDM (GFDM) where one CP is used instead of transmitting CP again and again, thereby increasing the spectral efficiency. In [15] DST has been used instead of DFT along with known sequences as guard band to speed up the process.

The major focus of the improvements is to use known sequence in the guard band so that the information can be used for channel estimation at the receiver. Another focus area is methods to

reduce the PAPR. The different techniques have been discussed in Chapter 2. Taking motivation from the efforts, a comparative study has been done on performance of OFDM system by using DCT and DST as spreading transforms. The advantage of these transforms is that these have real transformation matrix and thus do not require complex arithmetic as in case of DFT or IFFT.

1.3 THESIS ORGANIZATION

The thesis has been organized as follows

CHAPTER 2 introduces the OFDM scheme and the problems related to it

CHAPTER 3 introduces the DFT-s-OFDM scheme and various spreading algorithms

CHAPTER 4 introduces the various transforms which have been used

CHAPTER 5 gives the simulation results conclusion

CHAPTER 6 summarizes the thesis and presents future work.

CHAPTER 2

OFDM: A MULTI-CARRIER MODULATION SYSTEM

2.1 INTRODUCTION TO OFDM

The coherence bandwidth B_c is in the range of 200-300 KHz. When the transmission bandwidth is greater than the coherence bandwidth then channel is frequency selective and leads to the problem of ‘fading’. Suppose transmission bandwidth is 1024 KHz then there will be ISI in time domain. But in a MC system if we have 256 sub-carriers then the bandwidth of each sub-carrier will be 4 KHz which is much less than coherence bandwidth. Thus, these sub-carriers experience ‘flat-fading’ and hence there is no ISI. Thus, a Multi-Carrier Modulation System (MCMS) is good alternative over Single-Carrier system. A MCMS is shown in Fig. 2.1

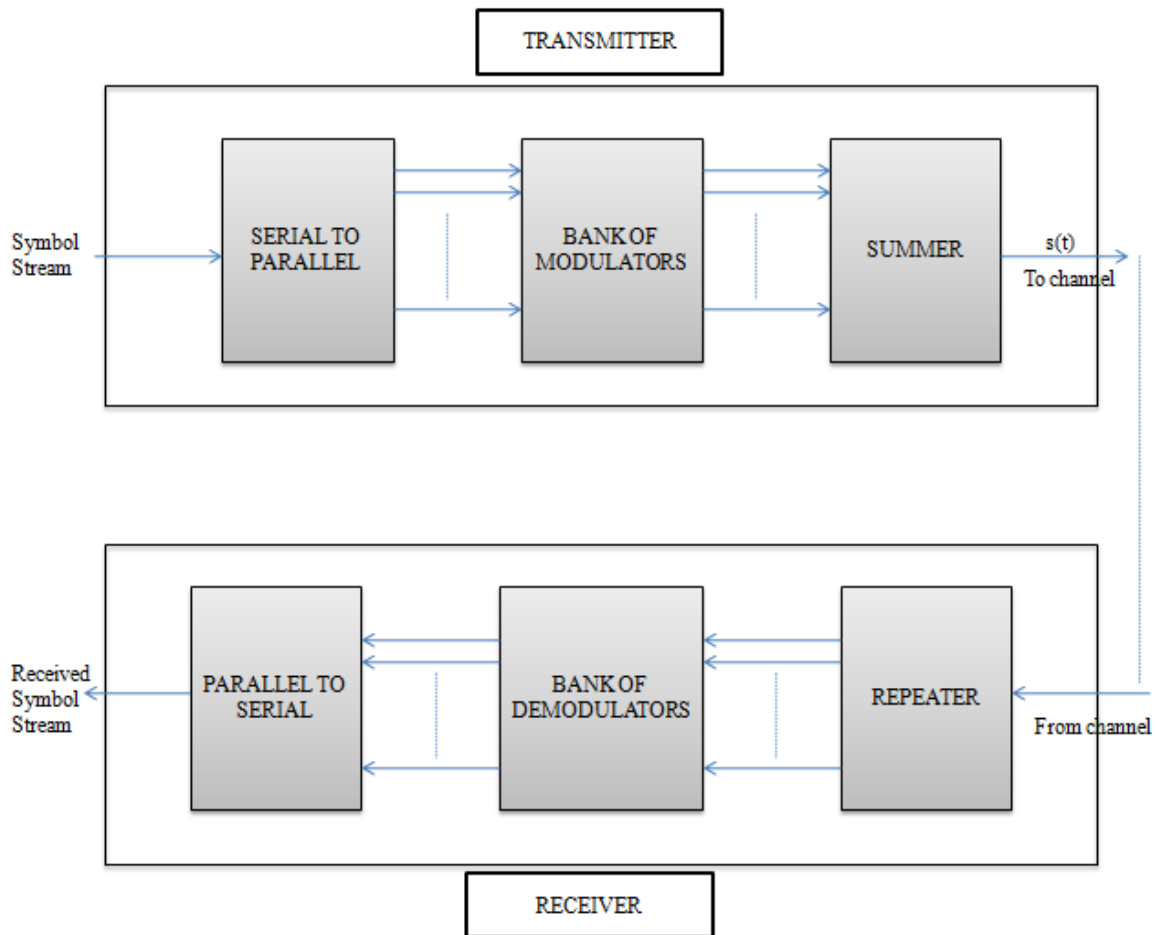


Fig. 2.1 : Multi-Carrier Multiplexing System

The MCMS transmits N symbols using N sub-carriers in time period $\frac{N}{B}$. Thus, the symbol rate is given as $\frac{N}{N/B}$ which is equal to B which is same as that of single carrier systems. The symbol duration of MCMS symbol is N times the symbol duration of single carrier system as shown in Fig. 2.2

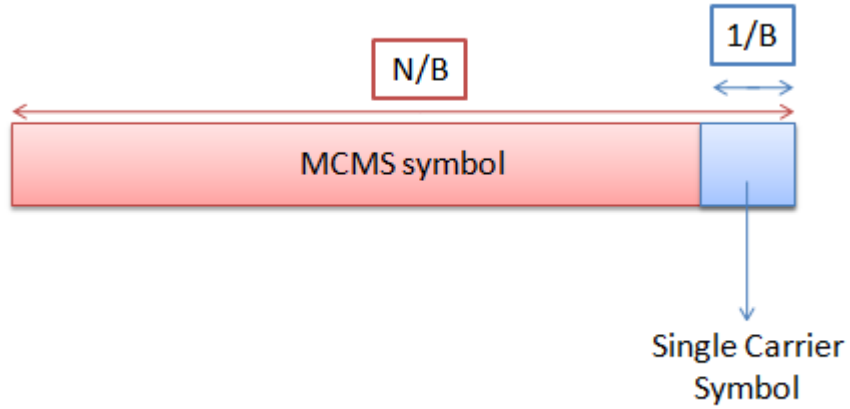


Fig. 2.2 : Comparison of symbol duration for MC and SC systems

As seen in the Fig. 2.1 a MCMS requires a bank of modulators and demodulators at transmitter and receiver respectively. This is one of the biggest drawbacks of a MCMS as design of bank of modulators and demodulators is very complex. This problem was solved in 1971 by Weinstein and Ebert in their paper [3] ‘Data Transmission by FDM using DFT’ which is also the basis for OFDM scheme. They proposed a scheme to bypass the use of bank of modulators and demodulators by use the IDFT and DFT for modulation and demodulation.

For a MCMS with a transmission bandwidth B and number of sub-carriers N the i^{th} data stream represented by symbol X_i is modulated by sub-carrier f_i . The composite MCMS signal is given as $s(t) = \sum_i X_i e^{j2\pi f_i t}$. Here the i^{th} sub-carrier $f_i = i \frac{B}{N}$. Thus, the signal is given by Equation (2.1)

$$s(t) = \sum_i X_i e^{j2\pi i \frac{B}{N} t} \quad (2.1)$$

Now if this signal is sampled at Nyquist sampling rate i.e. B (the sampling time T_s is $\frac{1}{B}$), then the u^{th} sample is given by Equation (2.2)

$$s(uT_s) = \sum_i X_i e^{j2\pi \frac{iu}{N}} \quad (2.2)$$

The Equation 2.2 resembles the IDFT of the symbols $X_i \in [X(0) \ X(1) \ \dots \ X(N-1)]$. Thus, we do not require bank of modulators. By considering the sampled signal we get that the samples which are the IDFT of the information symbols. Thus the OFDM signal can be generated by taking the IDFT of the information symbols. At the receiver the demodulation is done by employing the DFT on the received signal. This scheme of generating the MC signal is known as OFDM. An even less complex way of implementation is by using FFT and IFFT instead of DFT and IDFT respectively. The block diagram of an OFDM system is shown in Fig. 2.3

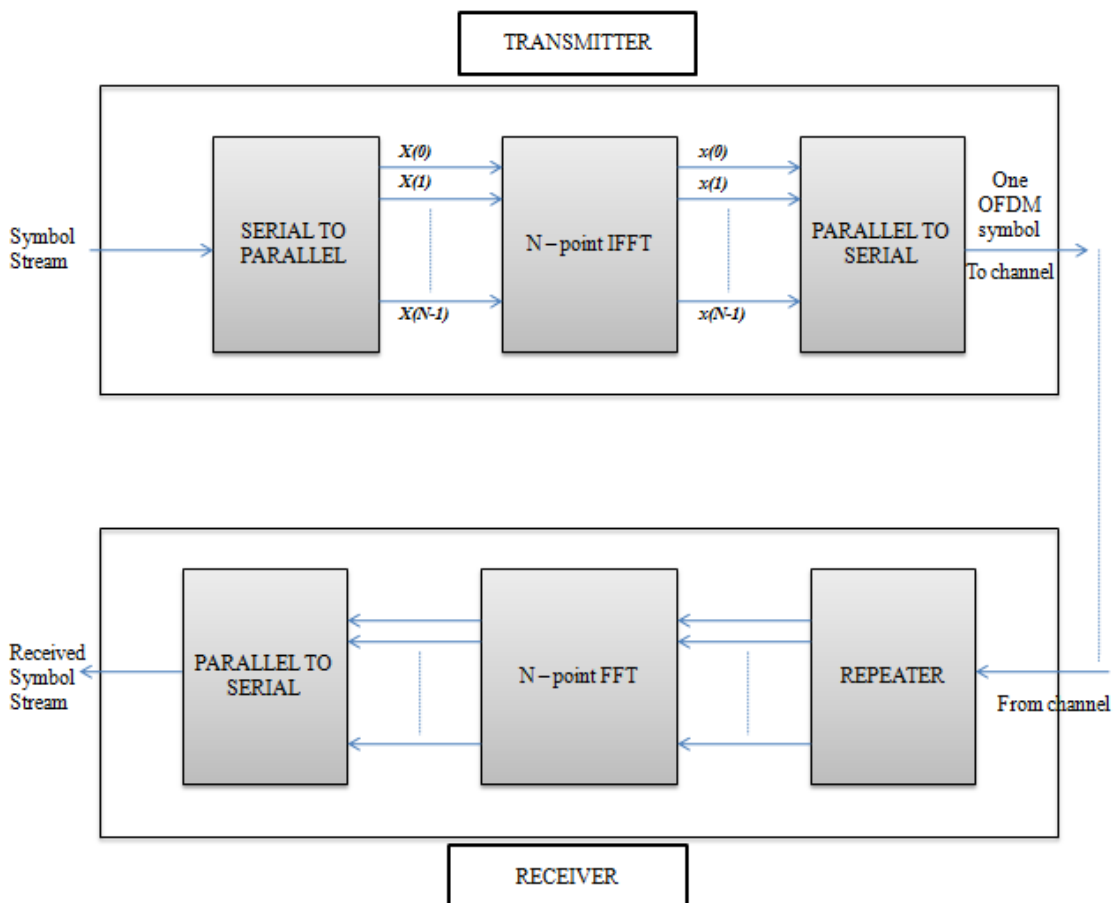


Fig. 2.3 : Block diagram of OFDM system

Many such OFDM symbols are transmitted over the channel as shown in Fig. 2.4. In case of a frequency selective channel generally modeled as a multi-tapped channel there may be Inter-Symbol-Interference for such symbol arrangement.

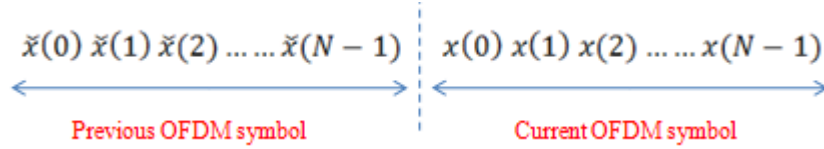


Fig. 2.4 : OFDM symbol without Cyclic-Prefix

If the symbols are passed through an L-tap channel then sub-carrier at the receiver contain information from previous symbol, again leading to ISI. This is illustrated in Equations (2.3) for first subcarrier. Similarly L-1 sub-carriers will have some component of the previous symbol.

$$y(0) = h(0)x(0) + h(1)\tilde{x}(N - 1) + h(2)\tilde{x}(N - 2) \dots \dots + h(L - 1)\tilde{x}(N - L + 1) \quad (2.3)$$

This can be overcome by the addition of Cyclic-Prefix i.e. a small portion of current symbol is added as prefix to overcome the effect of ISI channel. This is done as shown in Fig. 2.5

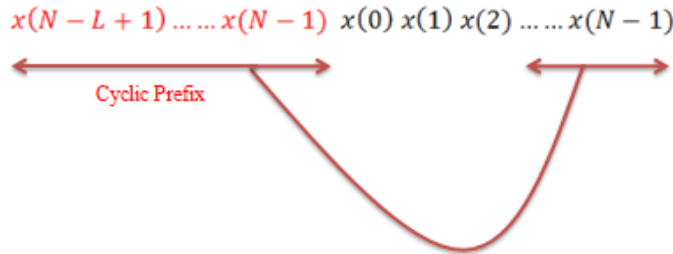


Fig. 2.5 : Addition of Cyclic-Prefix

The Equation (2.4) represents what is received for first sub-carrier at the receiver.

$$y(0) = h(0)x(0) + h(1)x(N - 1) + h(2)x(N - 2) \dots \dots + h(L - 1)x(N - L + 1) \quad (2.4)$$

For any arbitrary sub-carrier this simplifies to a circular convolution. Thus, the relation between the symbol sent over the l^{th} channel and what is received at the receiver in the frequency domain is given as in Equation (2.5) where $Y(l)$ represents the N-point DFT of the symbol $y(.)$ obtained at the receiver, $X(l)$ represents the N-point DFT of the symbol $x(.)$ sent

over the channel, $H(l)$ represents the N-point DFT of the channel impulse response $h(.)$ after zero padding of N-L zeros and $V(l)$ represents the N-point DFT of the AWGN noise introduced by the channel

$$Y(l) = H(l)X(l) + V(l) \quad (2.5)$$

The effect of adding this cyclic-prefix is conversion of wideband frequency channel into a number of parallel flat-fading channels as it is evident from Equation (2.5) that information obtained at each sub-carrier is independent of what is sent over other sub-carrier. Thus, we get N parallel flat-fading channels as depicted in Fig. 2.6

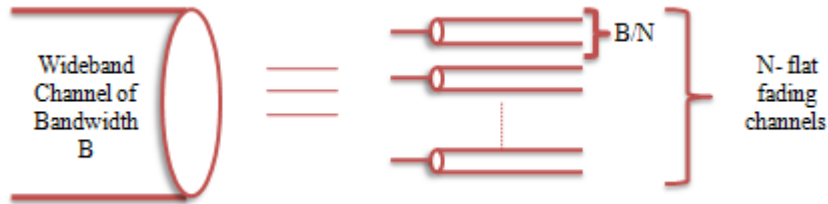


Fig. 2.6 : Effect of adding Cyclic-Prefix

Thus, the OFDM symbol consists of the sequence obtained after the information symbols are passed from N-point IFFT and then as shown a cyclic-prefix (CP) is added. This CP is added to mitigate the effect of frequency selective channel. Such a scheme is known as Cyclic-Prefix OFDM or CP-OFDM.

The addition of cyclic-prefix is necessary but it leads to loss of spectral efficiency as redundant data is sent. This loss in efficiency is given as in Equation 2.6

$$\text{Loss} = \frac{L - 1}{N + L - 1} \quad (2.6)$$

A typical WiMAX system has 256 sub-carriers and sub-carrier bandwidth of 15.625 kHz. Thus, the bandwidth is 4 MHz and the OFDM symbol time without CP is 64 μ s. The CP length is taken as 12.5 % i.e. 8 μ s in this case giving an CP-OFDM symbol time of 72 μ s. The number of samples is given as $\frac{\text{Symbol duration}}{\text{Sample Time}}$ and thus, $L = 32$ and $N = 256$ giving a spectral loss of 11.1% due addition of CP.

The schematic of CP-OFDM scheme is shown in Fig. 2.7. The new blocks at the transmitter side is the Addition of CP block. At the receiver the CP is removed and a detection scheme is needed to take into account the effect of ISI channel. The detection schemes which can achieve this are Zero-forcing, matched filter detection or MMSE detection.

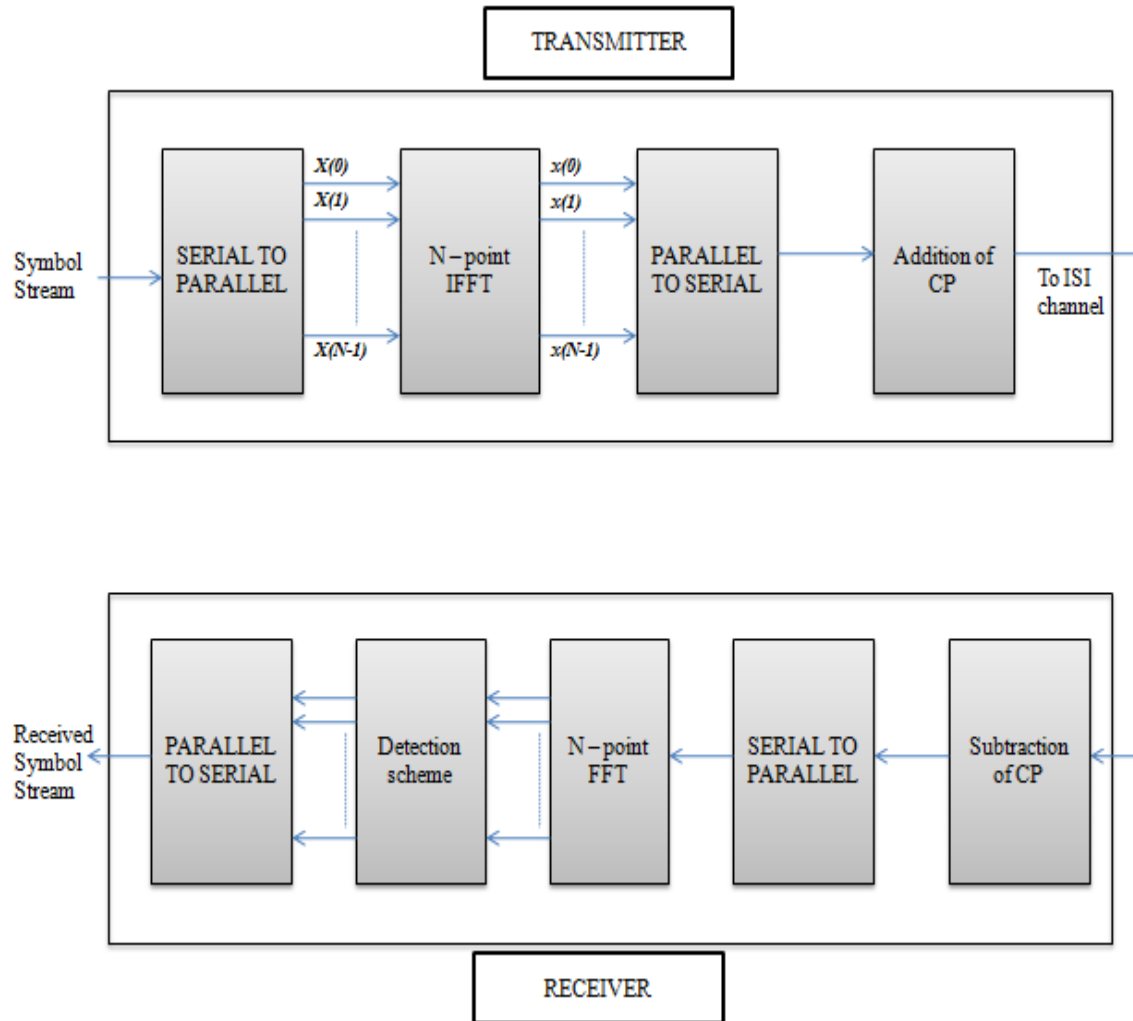


Fig. 2.7 : Block diagram of CP-OFDM system

2.2 DRAWBACKS OF OFDM

2.2.1 Effect of frequency Offset

One of the major drawbacks of OFDM system is the need for precise carrier synchronization at the receiver. If at the receiver the sampling instant is a little off, the problem of Inter-Carrier Interference creeps in and leads to reduction in SINR.

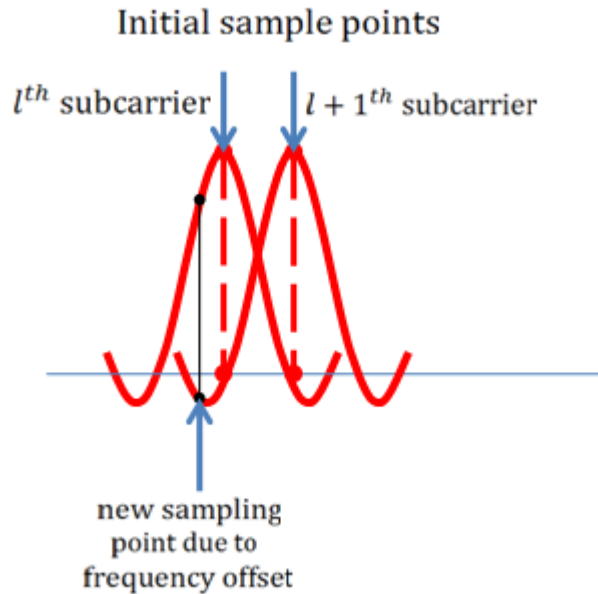


Fig. 2.8 : Effect of Carrier Frequency Offset

If there is perfect synchronization then the samples which the receiver picks contain no interference from adjacent sub-carriers. This can be seen in Fig. 2.8. However if there is a offset in carrier frequency then sample point shifts and some information from adjacent carrier is also picked leading to Inter-Carrier Interference. This effect is known as Carrier Frequency Offset (CFO). Even a small offset results in a large degradation in SNR. This effect is illustrated using an example.

For a system with bandwidth B and N sub-carriers, suppose the frequency offset is Δf such that $\frac{\Delta f}{B/N} = \epsilon$. The received signal $y(n)$ in this case is given as in Equation (2.7)

$$y(n) = \frac{1}{N} \sum_{k=-N/2}^{N/2} X_k H_k e^{\frac{j2\pi n(k+\epsilon)}{N}} + w_n \quad (2.7)$$

If there is no CFO then on taking the FFT we get the relation for each sub-carrier as given in Equation 2.5. However, if $\epsilon \neq 0$ then on taking the DFT of Equation (2.7) we get expression as in Equation (2.8)

$$Y_l = \frac{1}{N} \sum_n \sum_{k=-N/2}^{N/2} X_k H_k e^{\frac{j2\pi n(k-l+\epsilon)}{N}} + w_n \quad (2.8)$$

After some manipulation the Equation (2.8) reduces to the form as in Equation (2.9).

$$Y_l = H_l X_l \frac{\sin \pi \epsilon}{\sin \frac{\pi \epsilon}{N}} \frac{1}{N} e^{j\tilde{\phi}_l} + \sum_{k=-N/2}^{N/2} H_k X_k \left(\frac{\sin \pi \epsilon}{N \sin \pi \frac{l-k+\epsilon}{N}} \right) e^{j\tilde{\phi}_k} + V_l \quad (2.9)$$

This contains the desired signal part $\left(H_l X_l \frac{\sin \pi \epsilon}{\sin \frac{\pi \epsilon}{N}} \frac{1}{N} e^{j\tilde{\phi}_l} \right)$ (for $k = l$ case) and also interference

from $\left(I_l = \sum_{k=-N/2}^{N/2} H_k X_k \left(\frac{\sin \pi \epsilon}{N \sin \pi \frac{l-k+\epsilon}{N}} \right) e^{j\tilde{\phi}_k} \right)$ other sub-carriers for ($k \neq l$). In this case we

measure SINR which is given as $\frac{\text{Signal Power}}{\text{Noise Power} + \text{Interference Power}}$. On solving we get the expression as Equation (2.10) where P is the signal power, H is the average gain across sub-carrier and σ_n^2 is the noise power. This expression is for the case of $N \rightarrow \infty$.

$$\text{SINR} = \frac{P|H|^2 \left(\frac{\sin \pi \epsilon}{\pi \epsilon} \right)^2}{0.822(\sin \pi \epsilon)^2 + \sigma_n^2} \quad (2.10)$$

Considering $P = 10$ dB and $\sigma_n^2 = 0$ dB and taking the case of $\epsilon = 0$ i.e. no CFO the expression reduces to $\text{SNR} = 10$ dB. Now if $\epsilon = 0.05$, the value of SINR is 8.25 dB i.e. a reduction of 1.75 dB or 17% reduction. For the case of WiMAX the sub-carrier bandwidth is 15.625 KHz and a CFO of $\epsilon = 0.05$ means an offset of 0.78 KHz. For a carrier frequency of 2.4 GHz this offset means 0.0325×10^{-3} part of fraction. Thus, a very small fraction of CFO leads to 17% reduction in SNR. Thus, carrier synchronization is very critical aspect of OFDM systems. The CFO estimation can be done in time domain cyclic-prefix or training pilots are used [16]. CFO estimation can also be done in frequency domain as proposed by Moose [17] or Classen [18].

2.2.2 Problem of high PAPR

OFDM systems have high PAPR i.e. Peak to Average Power Ratio. PAPR is an important measure as it plays a role in design of power amplifiers. The power amplifiers are designed such that it operates in the middle point of the linear region such that variations don't force the amplifier to saturation region. This in turn leads to loss of orthogonality as distortion occurs resulting in creation of harmonics. This leads to Inter Carrier Interference. If PAPR is less this means that the signal has less variation about its mean value and thus, operates in the linear region of the amplifier

The PAPR for single-carrier system with BPSK is 1 or 0 dB. In an OFDM system modulation by BPSK scheme gives symbols as $-a$ or a . These values are loaded on to carriers via IFFT operation. The samples $x(k)$ are IFFTs of the BPSK symbols and thus, the average power is given by Equation (2.11)

$$E\{|x(k)|^2\} = \frac{1}{N^2} \sum_{i=0}^{N-1} E(|x_i|^2) \quad (2.11)$$

The power of individual symbols is $E(|x_i|^2) = a^2$ and thus, the average value $E(|x(k)|^2) = \frac{a^2}{N}$. The peak power is a^2 . Thus, $\text{PAPR} = \frac{a^2}{a^2/N} = N$ i.e. increases linearly with increase of number of sub-carriers.

There are many methods to decrease the PAPR. The PAPR reduction techniques are classified into different approaches. The clipping technique [19, 20] basically clips the peaks to reduce the PAPR. Another method is to use codeword [21, 22 and 23] for reduction of PAPR. Some probabilistic techniques are also used for this purpose. This problem of PAPR is also solved by spreading the energy of the symbols over the sub-carriers. This technique of reducing the PAPR by spreading of the symbol energy is called Discrete Fourier Transform-spreading-OFDM (DFT-s-OFDM) or commonly called Single-Carrier FDMA (SC-FDMA) [24-27]

CHAPTER 3

DFT-s-OFDM

3.1 INTRODUCTION TO SC-FDMA

The problem of high PAPR has been introduced because of the IFFT block in the transmitter. If at the transmitter we introduce N-point FFT block before the N-point IFFT block then the net effect of these two blocks is that they cancel out each other. This effectively reduced the multi-carrier system to a single carrier system and thus, PAPR comes out to be 1 or 0 dB. But this had reduced the system to a single carrier which has severe frequency selective channel related problems. One alternative is to use an M-point FFT block where $M < N$ which is essentially a trade-off between OFDM and SC-FDMA. This scheme is known as DFT-s-OFDM. The terms SC-FDMA and DFT-s-OFDM can be used interchangeably. The transmission and receiver scheme is shown in Fig 3.1

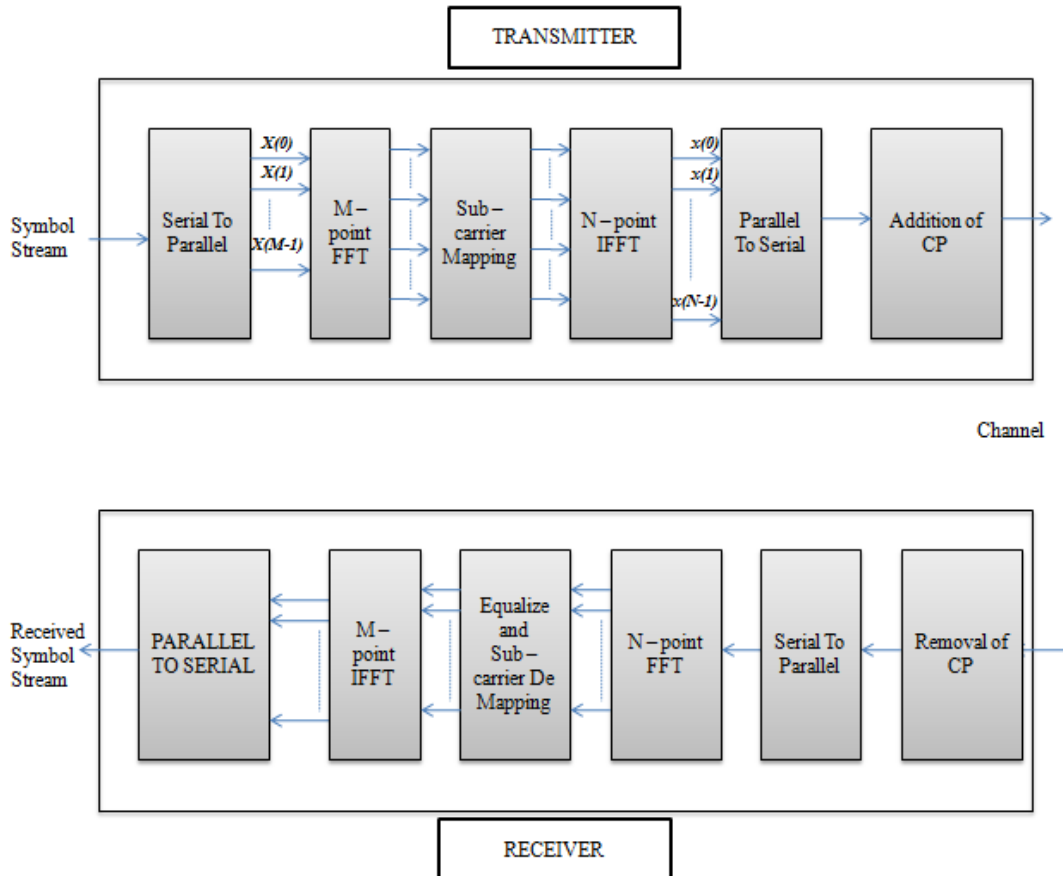


Fig. 3.1 : Block diagram of DFT-s-OFDM system

3.2 INTRODUCTION TO DFT-s-OFDM

DFT-s-OFDM helps in overcoming the high PAPR problem of an OFDM scheme. This scheme effectively reduces the PAPR and is still a multi-carrier scheme. Here the effective numbers of symbols which are loaded on the sub-carriers are less than that which is loaded in OFDM. In this scheme M symbols are first passed through an M -point DFT and then these are mapped onto N sub-carrier. This distributes the symbol energy of M symbols over N sub-carriers and as such is called DFT-spread-OFDM.

The sub-carrier mapping block is an important block in this scheme and depending on how mapping is done different schemes originate namely Interleaved FDMA (IFDMA), Localized FDMA (LFDMA) and Distributed FDMA (DFDMA). The sub-carrier mapping is done differently in these cases leading to different effects on PAPR reduction.

The different spreading techniques are illustrated using an example. Consider the value of $M = 4$ and $N = 16$ and 5 symbols which have been passed through 4-point DFT block. The four symbols are $(x(0) \ x(1) \ x(2) \ x(3))$ and the corresponding output of the DFT block is $(X(0) \ X(1) \ X(2) \ X(3))$ then the different spreading schemes are illustrated in Fig 3.2 through 3.4. When the mapping is done such that the DFT-block output is spread evenly over sub-carriers with equal spacing then the technique is called IFDMA. In this scheme between M DFT outputs $\frac{N}{M} - 1$ virtual carriers or sub-carriers with no information are inserted (these are represented by 0's in the diagram)

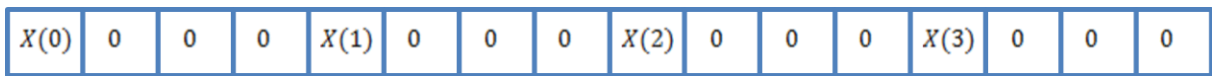


Fig. 3.2 : IFDMA mapping

In DFDMA scheme the M outputs from DFT-block are placed alternatively with no information sub-carriers as shown for initial $2 \times M$ sub-carriers. The remaining $N - 2 \times M$ sub-carriers are again virtual sub-carriers

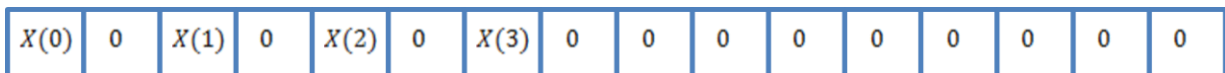


Fig. 3.3 : DFDMA mapping

In LFDMA the M DFT-block outputs are loaded into initial M sub-carriers and rest sub-carriers are virtual carriers.

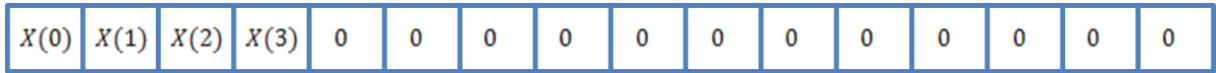


Fig. 3.4 : LFDMA mapping

The different spreading algorithms effect the PAPR differently as the IFFT output for these cases is different.

3.3 TIME DOMAIN REPRESENTATION OF DIFFERENT SPREADING TECHNIQUES

The modulated symbols $x(m)$ after passing through the M-point FFT block $X(l)$ are loaded on the sub-carrier, which in turn acts as input to the N-point IFFT. Thus, depending on the spreading algorithm the IFFT block output is different for the three cases. These are analyzed in the subsequent section. The relation between $x(m)$ and $X(l)$ is given by Equation (3.1)

$$X(l) = \sum_{r=0}^{M-1} x(r) e^{-\frac{j2\pi rl}{M}} \quad (3.1)$$

3.3.1 Time Domain representation of IFDMA

The input symbol sequence $x(m)$ is first passed through M-point DFT block. The output of the DFT block is denoted by $X(l)$. The IFDMA technique has a spreading factor $L = \frac{N}{M}$ then the output after carrier sub-mapping is given as in Equation (3.2)

$$X_{\text{IFDMA}}(k) = \begin{cases} X\left(\frac{k}{L}\right) & \text{if } k = pl \text{ where } p = 0, 1, \dots, M-1 \\ 0 & \text{if } k \neq pl \end{cases} \quad (3.2)$$

This is fed to the input of the N-point FFT block. The output $x_{\text{IFDMA}}(n)$ of the IFFT block is given by Equation (3.2) where $n = Ml + m$ and $l = 0, 1, \dots, L - 1$ and $m = 0, 1, \dots, M - 1$

$$x_{\text{IFDMA}}(n) = \frac{1}{N} \sum_{k=0}^{N-1} X_{\text{IFDMA}}(k) e^{\frac{j2\pi kn}{N}} \quad (3.3)$$

Substituting the values for k , N and n we get the expression as in Equation (3.3)

$$x_{\text{IFDMA}}(n) = \frac{1}{LM} \sum_{p=0}^{M-1} X(p) e^{\frac{j2\pi(Ml+m)p}{M}} \quad (3.4)$$

On further simplification the expression reduces to $x_{\text{IFDMA}}(n) = \frac{1}{LM} \sum_{p=0}^{M-1} X(p) e^{\frac{j2\pi mp}{M}} = \frac{1}{L} \text{IDFT}(X(p))$. Thus, the expression for output for IFFT block in the case of IFDMA is reduced to form as in Equation (3.4)

$$x_{\text{IFDMA}}(n) = \frac{1}{L} x(m) \quad (3.5)$$

Thus, in the case of IFDMA the signal obtained is a scaled version of the original signal as in Equation (3.5). This is the reason for reduction of PAPR in case of IFDMA.

3.3.2 Time Domain representation of DFDMA

The input symbol sequence $x(m)$ is first passed through M-point DFT block. The output of the DFT block is denoted by $X(l)$. In this scheme initially DFT output are loaded alternatively with carriers having no information and the rest are also virtual sub-carriers. Thus, the effect is that the IFFT output has a phase term in it as in Equation (3.6)

$$x_{\text{DFDMA}}(n) = \frac{1}{L} e^{j2\pi rn} x(m) \quad (3.6)$$

3.3.3 Time Domain representation of LFDMA

The input symbol sequence $x(m)$ is first passed through M-point DFT block. The output of the DFT block is denoted by $X(l)$. The IFDMA technique has all the DFT outputs in the initial sub-carriers and rest are virtual carriers.

$$X_{\text{LFDMA}}(k) = \begin{cases} X(k) & \text{if } k = 0, 1, \dots, M-1 \\ 0 & \text{if } k > M-1 \end{cases} \quad (3.7)$$

This is fed to the input of the N-point FFT block. The output $x_{\text{LFDMA}}(n)$ of the IFFT block is given by Equation (3.8) where $n = Lm + l$ and $l = 0, 1, \dots, L-1$ and $m = 0, 1, \dots, M-1$

$$x_{\text{LFDMA}}(n) = \frac{1}{N} \sum_{k=0}^{N-1} X_{\text{LFDMA}}(k) e^{j2\pi kn} \quad (3.8)$$

Substituting the values for N and n we get the expression as in Equation (3.9)

$$x_{\text{LFDMA}}(n) = \frac{1}{LM} \sum_{p=0}^{N-1} X_{\text{LFDMA}}(k) e^{j2\pi k(Lm+l)p} \quad (3.9)$$

There are two cases for Equation (3.9). The case for $l = 0$ yields $x_{\text{LFDMA}}(n) = \frac{1}{L} x(m)$ and $l =$ non-zero yields (3.10)

$$x_{\text{LFDMA}}(n) = \frac{1}{LM} \sum_{p=0}^{M-1} X(k) e^{j2\pi k(Lm+l)p} \quad (3.10)$$

By using the relation in Equation (3.1) we get updated Equation (3.11)

$$x_{\text{LFDMA}}(n) = \frac{1}{LM} \sum_{p=0}^{M-1} \sum_{r=0}^{M-1} x(r) e^{-\frac{j2\pi rl}{M}} e^{\frac{j2\pi k(Lm+l)p}{M}} \quad (3.11)$$

On further modification we get the LFDMA IFFT output as in Equation (3.12)

$$x_{\text{LFDMA}}(n) = \frac{1}{LM} \sum_{r=0}^{N-1} \frac{x(r)}{1 - e^{j2\pi\{\frac{m-r}{M} + \frac{l}{LM}\}}} \quad (3.12)$$

The IFFT output for LFDMA is also a scaled version of the input but there is also a weighing factor associated. The following table summarizes the IFFT output for the three cases

Table 3.1: IFFT block output for different spreading algorithms

Spreading Technique	IFFT block output
IFDMA	$x_{\text{IFDMA}}(n) = \frac{1}{L} x(m)$
DFDMA	$x_{\text{DFDMA}}(n) = \frac{1}{L} e^{\frac{j2\pi rn}{N}} x(m)$
LFDMA	$x_{\text{LFDMA}}(n) = \frac{1}{LM} \sum_{r=0}^{N-1} \frac{x(r)}{1 - e^{j2\pi\{\frac{m-r}{M} + \frac{l}{LM}\}}}$

In all the cases the output is a scaled down version of the input signal. Thus, this helps in reducing the PAPR of the system. The reduction in PAPR is analyzed by plotting the complimentary cumulative distribution function (CCDF). The CCDF measures the probability that energy of the each symbol is greater than the average energy of the symbol frame.

CHAPTER 4

TRANSFORMS

4.1 INTROUCTION TO TRANSFORMS

The DFT and IDFT blocks are the backbone of an OFDM system. But the problem with DFT and its inverse is that the transformation involves complex sinusoids i.e. addition and multiplication of complex numbers. The Discrete Cosine Transform (DCT) [27] and Discrete Sine Transform (DST) [28] are also Fourier related transforms used in signal processing techniques. The main advantage of these transforms is that the basis vectors are real. As such these can also be used for spreading instead of DFT or FFT block.

These transforms are have been used and there effects are studied on BER and PAPR so that DCT and DST can be used instead of DFT. This will help in reducing the complexity as these do not involve complex numbers.

4.2 DISCRETE FOURIER TRANSFORM (DFT)

Discrete Fourier transform (DFT) is a mathematical concept which is used for Fourier analysis of finite-domain discrete-time signals. DFT has wide applications in signal processing and related fields. These are used to analyze the frequency content of a signal. The main advantage is that the DFT can be computed efficiently using the Fast Fourier transform (FFT) algorithm. The calculation of DFT takes $O(N^2)$ arithmetical operations. This can be reduced to $O(N \log N)$ operations by using the FFT algorithms

The FFT and DFT are used interchangeably in literature as FFT algorithms are commonly employed to compute the DFT. DFT actually refers to a mathematical transformation, while "FFT" refers to any one of several algorithms used for the computation of DFT.

The DFT of any sequence $x(n)$ is defined by Equation (4.1)

$$X(k) = \sum_{n=0}^{N-1} x(n)e^{-\frac{j2\pi kn}{N}} \quad k = 0,1,2 \dots N - 1 \quad (4.1)$$

The corresponding IDFT formula is given in Equation (4.2)

$$x(n) = \frac{1}{N} \sum_{k=0}^{N-1} X(k) e^{j2\pi kn/N} \quad n = 0, 1, 2 \dots N - 1 \quad (4.2)$$

The properties of DFT are summarized in Table 4.1

Table 4.1: Properties of DFT

	Property	Time Domain	Frequency Domain
1.	Linearity	$a x(n) + b h(n)$	$a X(k) + b H(k)$
2.	Circular time shift	$x((n - l))_N$	$X(k)e^{-j2\pi kl/N}$
3.	Circular frequency shift	$x(n)e^{j2\pi ln/N}$	$X((k - l))_N$
4.	Complex conjugate	$x^*(n)$	$X^*(N - k)$
5.	Circular convolution	$x(n) \otimes h(n)$	$X(k) H(k)$
6.	Multiplicity	$x(n)h(n)$	$\frac{1}{N} X(k) \otimes H^*(k)$
7.	Parseval's theorem	$\sum_{n=0}^{N-1} x(n)h^*(n)$	$\frac{1}{N} \sum_{n=0}^{N-1} X(k)H^*(k)$

DFT is discrete in both time and frequency domain and thus can be implemented by signal processors. The DFT is used extensively in Spectral analysis of signals [32, 33], audio processing, and data compression [35, 36 and 37] and many more applications. It is also used in mathematics for solving partial difference equations.

4.3 DISCRETE COSINE TRANSFORM (DCT)

A discrete cosine transform (DCT) is a Fourier-related transform which uses only real numbers. DCTs are equivalent to DFTs of roughly twice the data length and operate on real data with even symmetry. The discrete cosine transforms (DCTs) express a function or a signal in terms of a sum of sinusoids with different frequencies and amplitudes. The difference between DCT and DFT is that the DCT uses only cosine functions as basis vectors, whereas the DFT uses complex exponentials i.e. both cosines and sine's.

The DCT for a sequence $x(n)$ is defined as Equation (4.3)

$$X(k) = \sum_{n=0}^{N-1} x(n) \cos\left(\frac{2\pi nk}{N}\right) \quad (4.3)$$

The IDCT is given in Equation (4.4)

$$x(n) = \frac{1}{N} \sum_{k=0}^{N-1} X(k) \cos\left(\frac{2\pi nk}{N}\right) \quad (4.4)$$

The DCT has the property of concentrating the energy into lower frequency bands. This property of energy compaction is used for compression of speech and images and is used in standards like JPEG for picture compression [11] and MPEG for speech coding [13].

4.4 DISCRETE SINE TRANSFORM (DST)

The Discrete Sine transform (DST) is another transform which is Fourier-related. Like DCT it is similar to DFT with a purely real transformation matrix. DSTs are equivalent to DFTs of roughly twice the data length and operate on real data with odd symmetry. The DST expresses a function or a signal in terms of a sum of sinusoids with different frequencies and amplitudes. The difference between DCT and DST is that the DST uses only sine functions as basis vectors. The DST for a assigned sequence $x(n)$ is defined [29] as Equation (4.5)

$$X(k) = \sqrt{\frac{2}{N+1}} \sum_{n=0}^{N-1} x(n) \cos\left(\frac{\pi nk}{N+1}\right) \quad (4.5)$$

The IDST is given in Equation (4.6)

$$x(n) = \sqrt{\frac{2}{N+1}} \sum_{k=0}^{N-1} X(k) \cos\left(\frac{\pi nk}{N+1}\right) \quad (4.6)$$

The effect of using DCT and DST has been simulated and analyzed in the DFT-s-OFDM. These can called DCT-s-OFDM and DST-s-OFDM for the case of DCT and DST respectively

CHAPTER 5

SIMULATION AND RESULTS

5.1 SIMULATION MODEL FOR OFDM FOR AWGN CHANNEL

The software MATLAB has been used for simulation purpose. The simulation model used for CP - OFDM system in AWGN channel is shown in Fig 5.1

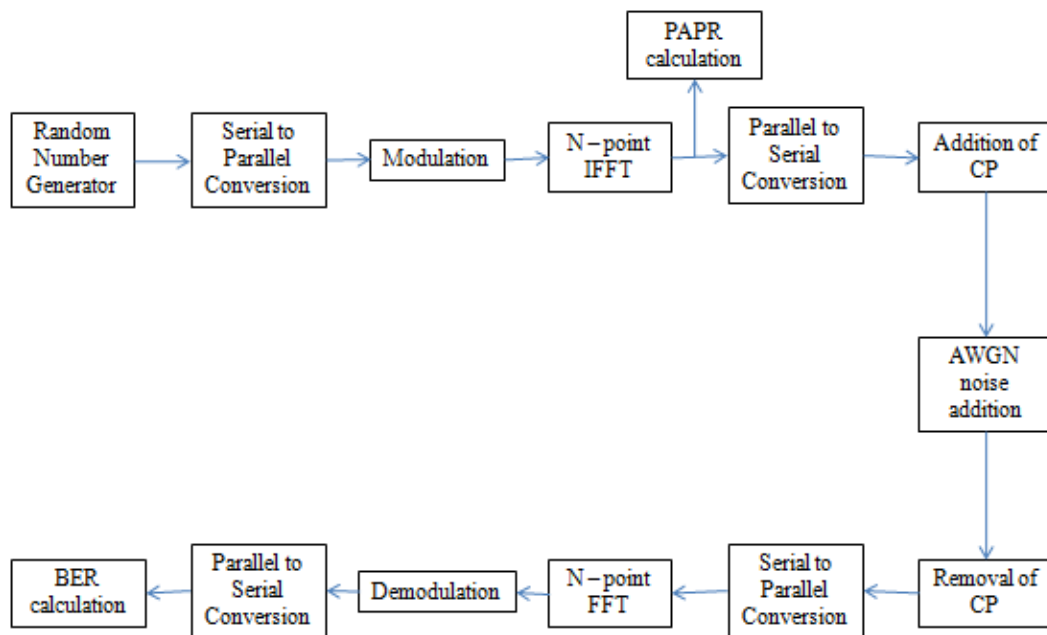


Fig. 5.1 OFDM simulation model

The parameters used for simulation purpose are given in Table 5.1

Table 5.1: Simulation parameters for OFDM system

Number of sub-carriers (N)	256
Cyclic Prefix length	64
Modulations used	QPSK, 16-QAM and 64-QAM
Number of frames	500

As seen in Fig 5.1 the random data is generated. Binary data is generated and corresponding to the modulation scheme used 2/4/6 binary data is sent in parallel to the modulator. The output of the modulator contains N symbols which are to be loaded on the sub-carriers. This block of N symbols constitute a frame. 500 such frames have been simulated to average out the bit error rate (BER) and the PAPR. The OFDM symbol is then generated by N-point IFFT of the frame and 25% cyclic prefix is added to generate the final OFDM frame.

The channel is AWGN and as such depending on the signal power noise is added for different values of SNR. At the receiver first the cyclic-prefix is removed and the result is passed through the N-point FFT block and demodulation is done to get the received symbols. Form this data BER is calculated for SNR values from 0 to 10 dB. The value of N is 256.

5.1.1 BER for QPSK

QPSK modulates 4 bits into one symbol. A single frame has (4×256) bits and 500 such frames are simulated. The BER results for QPSK modulation are as in Table 5.2

Table 5.2: BER v/s SNR values for QPSK

SNR	BER
0	0.159102
1	0.129734
2	0.104191
3	0.07898
4	0.056277
5	0.039184
6	0.023246
7	0.01277
8	0.006137
9	0.002336
10	0.000828

5.1.2 BER for 16-QAM

16-QAM modulates 16 bits into one symbol. A single frame has (16×256) and 500 such frames are simulated. The BER results for QPSK modulation are as in Table 5.3

Table 5.3: BER v/s SNR values for 16-QAM

SNR	BER
0	0.28695
1	0.26323
2	0.23737
3	0.21161
4	0.18747
5	0.16379
6	0.14126
7	0.11942
8	0.09861
9	0.07812
10	0.05862

5.1.3 BER for 64-QAM

64-QAM modulates 64 bits into one symbol. A single frame has (64×256) bits and 500 such frames are simulated. The BER results for QPSK modulation are as in Table 5.4

Table 5.4: BER v/s SNR values for 64-QAM

SNR	BER
0	0.36046
1	0.34203
2	0.32406
3	0.30478
4	0.28408
5	0.26238
6	0.24018
7	0.21694
8	0.19523
9	0.17304
10	0.15244

5.1.4 BER comparison for OFDM in AWGN channel

The BER values for OFDM using different modulation are given in tables 5.1-5.3. The following plot gives a comparison between different modulation schemes. As expected QPSK gives the best performance

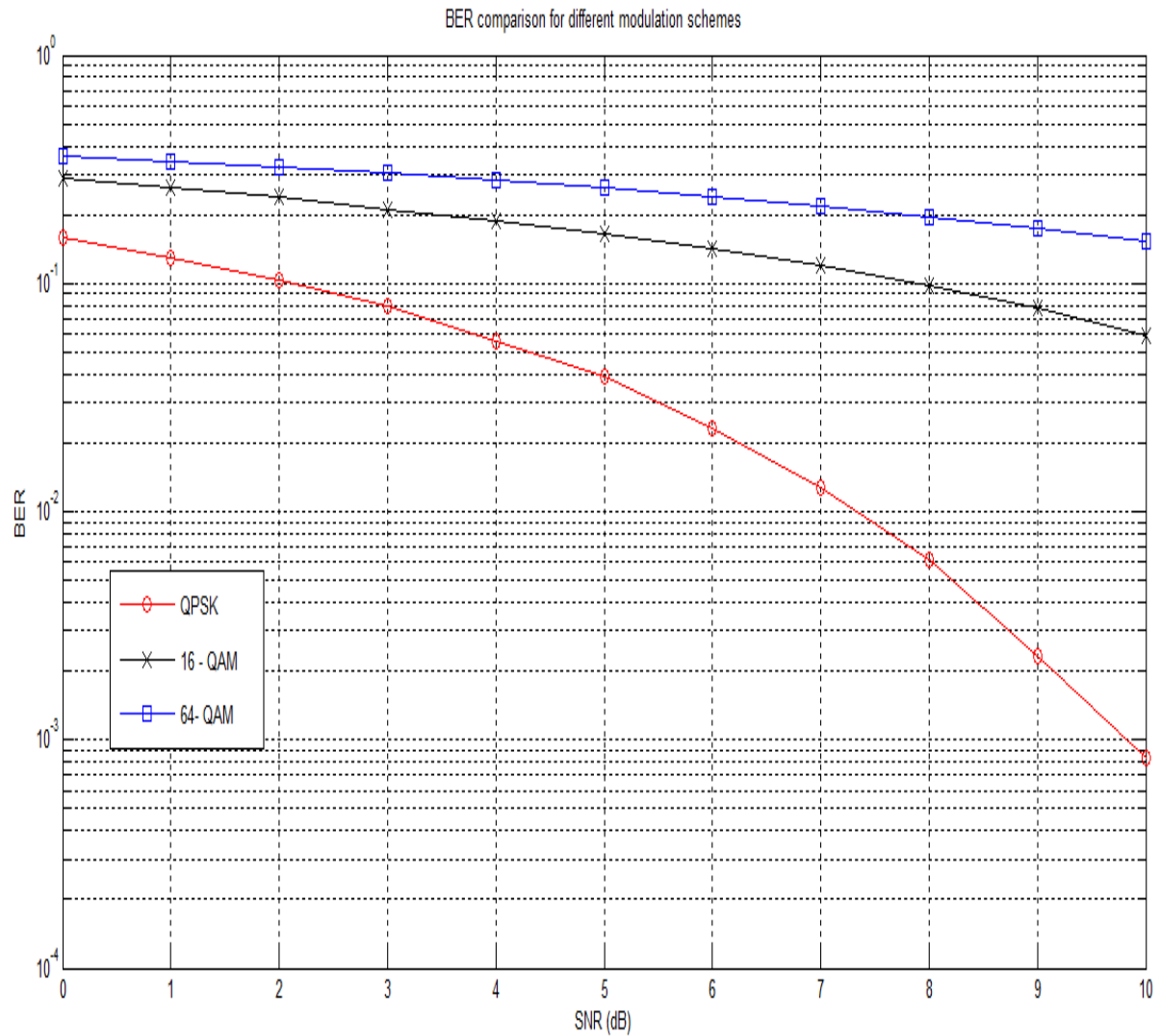


Fig. 5.2 : BER comparison for different modulation schemes

5.3 SIMULATION MODEL FOR DFT-s-OFDM IN AWGN CHANNEL

The simulation model used for DFT-s-OFDM for different spreading techniques in AWGN channel is shown in Fig 5.3

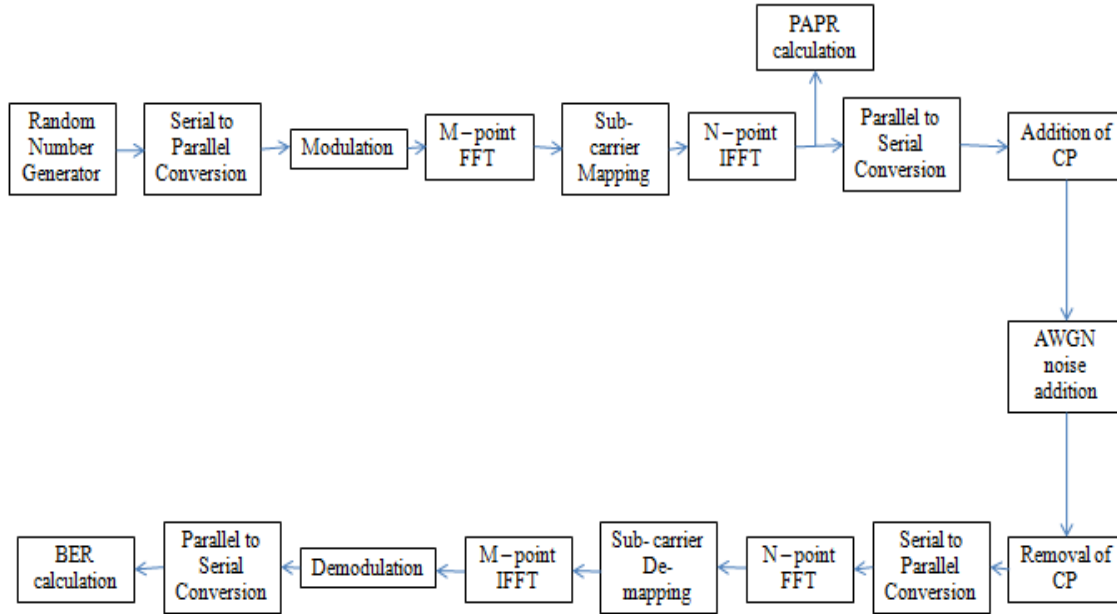


Fig. 5.3 : Simulation model for DFT-s-OFDM

The parameters used for simulation purpose are given in table 5.5

Table 5.5: Simulation parameters for DFT-s-OFDM

Number of sub-carriers (N)	256
M	64,128
Cyclic Prefix length	64
Modulations used	QPSK, 16-QAM and 64-QAM
Number of frames	500

As seen in Fig. 5.3 the random data is generated. Binary data is generated and corresponding to the modulation scheme used 2/4/6 binary data is sent in parallel to the modulator. The output of the modulator contains M symbols which are first sent to M-point FFT block for

spreading of the energy. These are then mapped to N subcarriers according to spreading technique discussed i.e. IFDMA, DFDMA and LFDMA. This block of N symbols constitute a frame. 500 such frames have been simulated to average out the bit error rate (BER) and the PAPR. The final symbol is then generated by N-point IFFT of the frame and 25% cyclic prefix is added to generate the final frame.

The channel is AWGN and as such depending on the signal power noise is added for different values of SNR. At the receiver first the cyclic-prefix is removed and the result is passed through the N-point FFT block followed by sub-carrier de mapping. The M-point IFFT block negates the effect of spreading and demodulation is done to get the received symbols. Form this data BER is calculated for SNR values from 0 to 10 dB. The value of N is 256.

5.3 SIMULATION RESULTS FOR LFDMA

5.3.1 BER for case M = 64

The BER values for different modulation schemes for the case when spreading factor is 4 is given in Table 5.6

Table 5.6: BER values for LFDMA with M = 64

SNR	QPSK	16-QAM	64-QAM
0	0.005789	0.035311	0.05991
1	0.003242	0.029504	0.054189
2	0.00159	0.02425	0.048125
3	0.000539	0.019246	0.043245
4	0.00018	0.01451	0.037639
5	4.30E-05	0.010416	0.033053
6	1.17E-05	0.0069	0.028344
7	3.91E-06	0.004211	0.024124
8	0	0.002313	0.020254
9	0	0.001176	0.015783
10	0	0.00048	0.012298

The BER v/s SNR plot for LFDMA for the case of M = 64 is plotted in Fig. 5.4

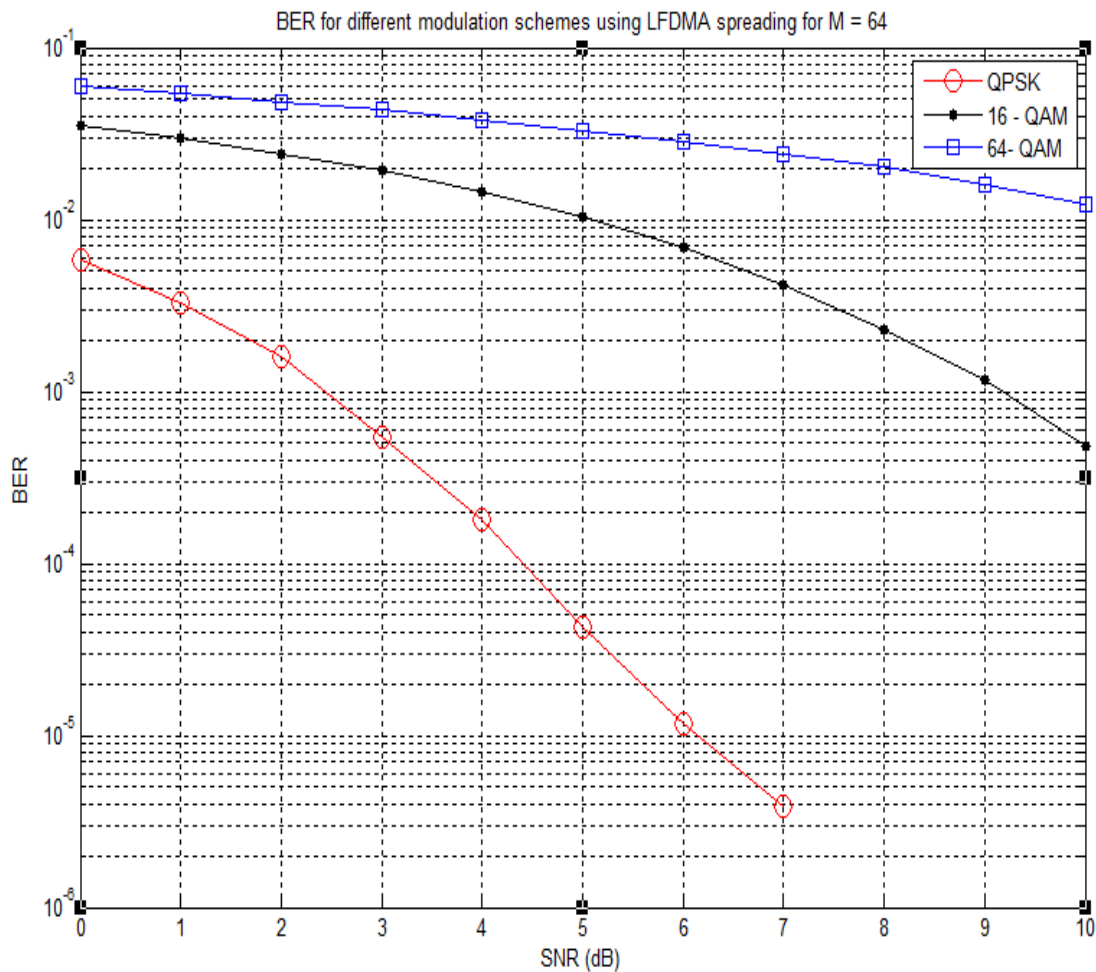


Fig. 5.4 : BER comparison for LFDMA with M = 64

5.3.2 BER for case M = 128

The BER values for different modulation schemes for the case when spreading factor is 2 is given in Table 5.7

Table 5.7: BER values for LFDMA with M = 128

SNR	QPSK	16-QAM	64-QAM
0	0.039352	0.106246	0.152918
1	0.028031	0.093695	0.142177
2	0.018875	0.082777	0.130803
3	0.01125	0.070799	0.119893
4	0.006137	0.059377	0.108335
5	0.002918	4.89E-02	0.097655

6	0.001184	3.82E-02	0.086022
7	0.000398	2.93E-02	0.076266
8	7.03E-05	0.020766	0.066229
9	1.95E-05	0.01368	0.05701
10	0	0.008428	0.048188

The BER v/s SNR plot for LFDMA for the case of $M = 128$ is plotted in Fig. 5.5

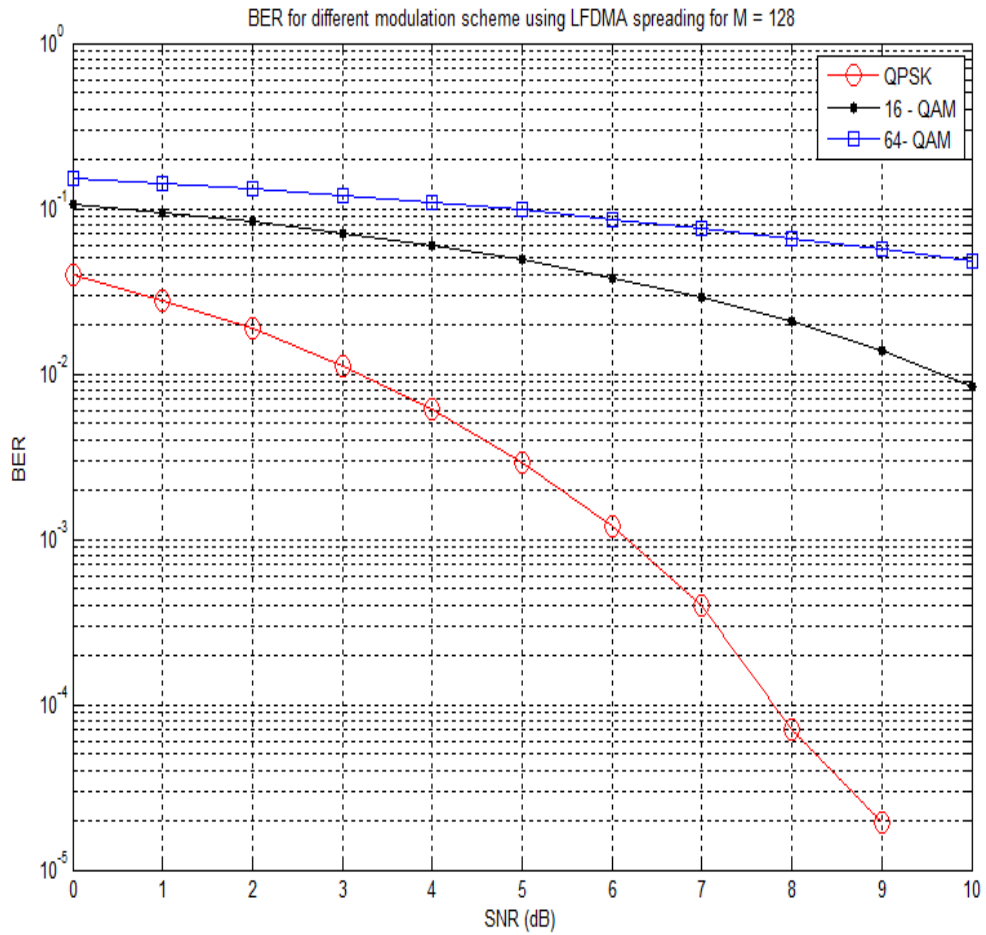


Fig. 5.5 : BER comparison for LFDMA with $M = 128$

The BER for QPSK is lowest in both the case using LFDMA spreading.

The BER comparison of LFDMA with OFDM for different modulation techniques is plotted in subsequent Fig. 5.6 through Fig. 5.8. Fig. 5.6 given the comparison for QPSK

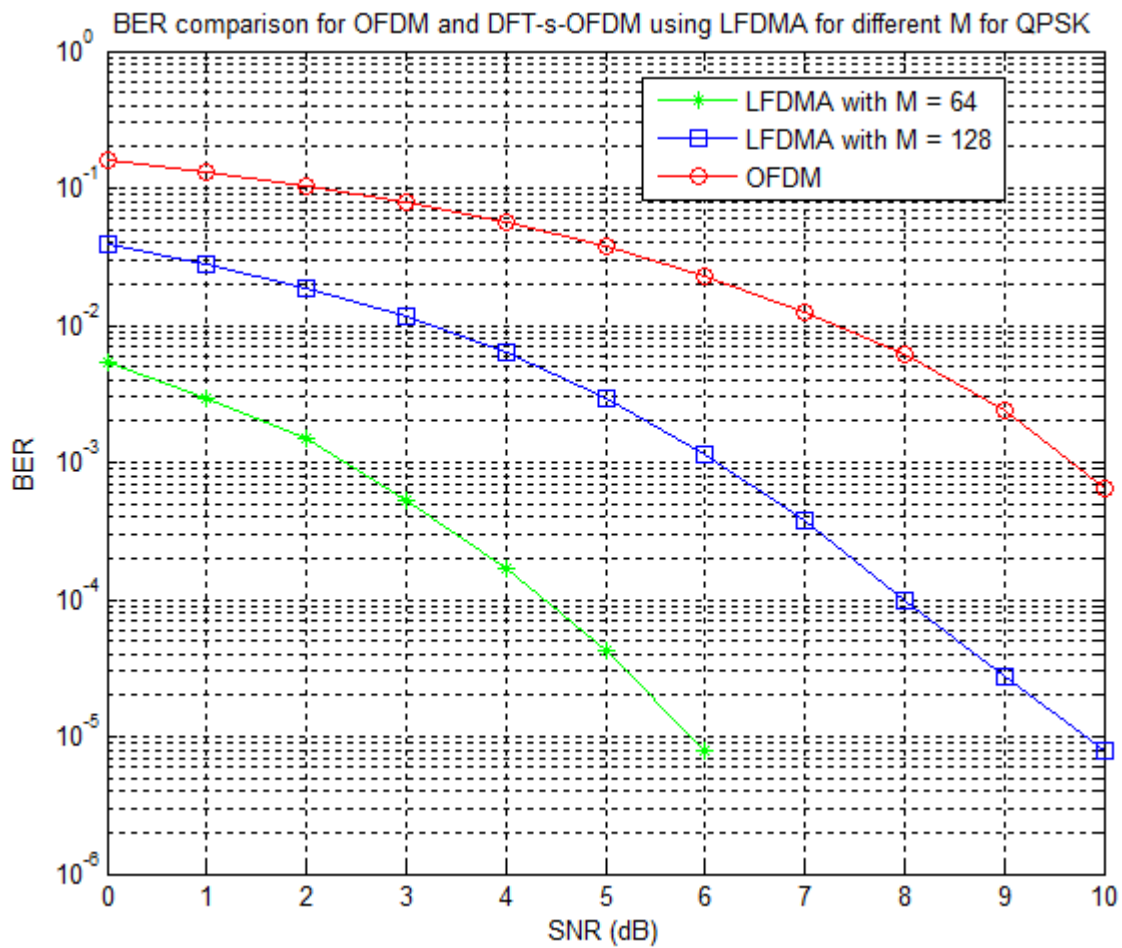


Fig. 5.6 : BER comparison of LFDMA and OFDM for QPSK

Fig. 5.7 given the comparison for 16-QAM between OFDM and LFDMA

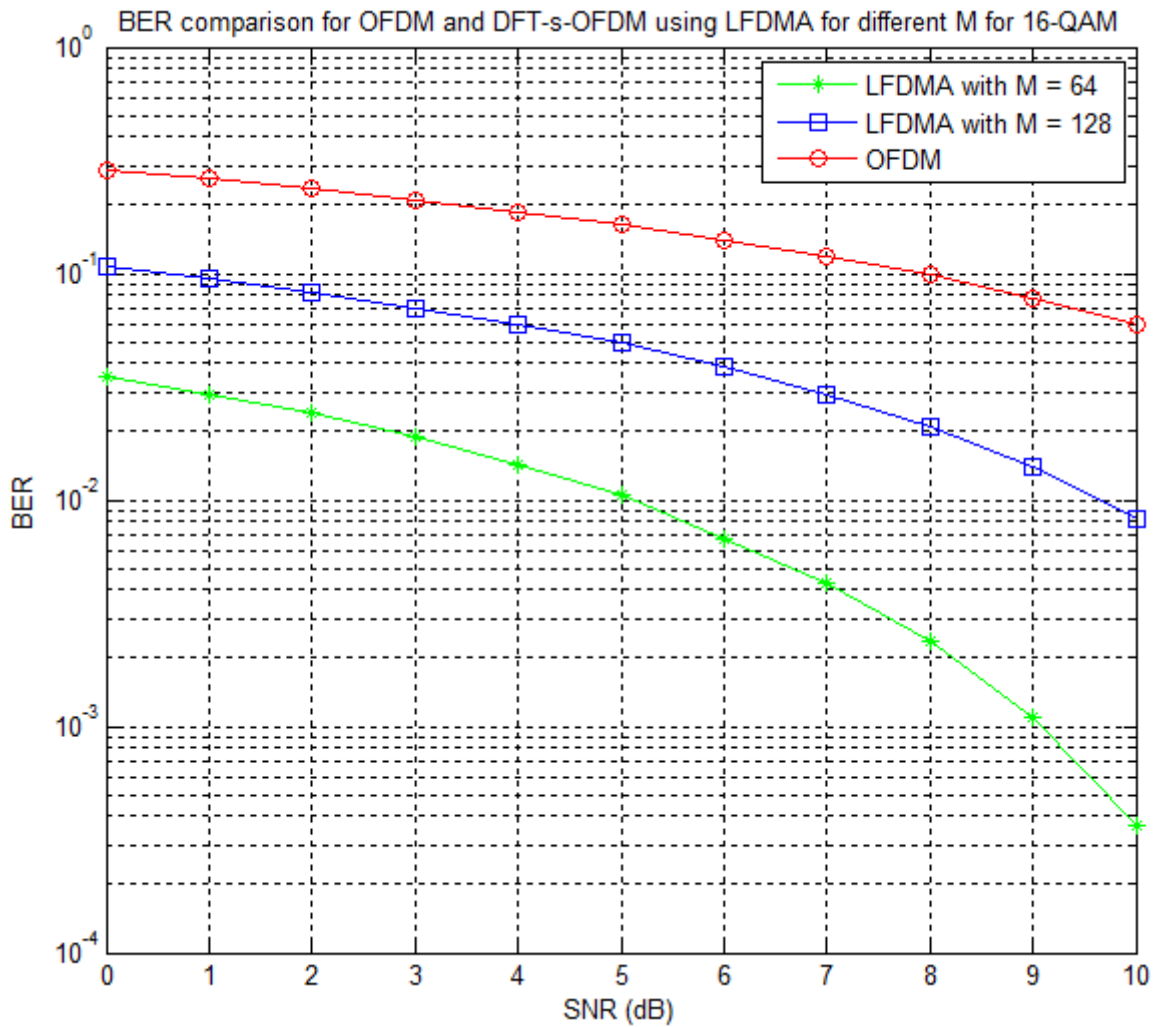


Fig. 5.7 : BER comparison of LFDMA and OFDM for 16-QAM

Fig. 5.8 given the comparison for 16-QAM between OFDM and LFDMA

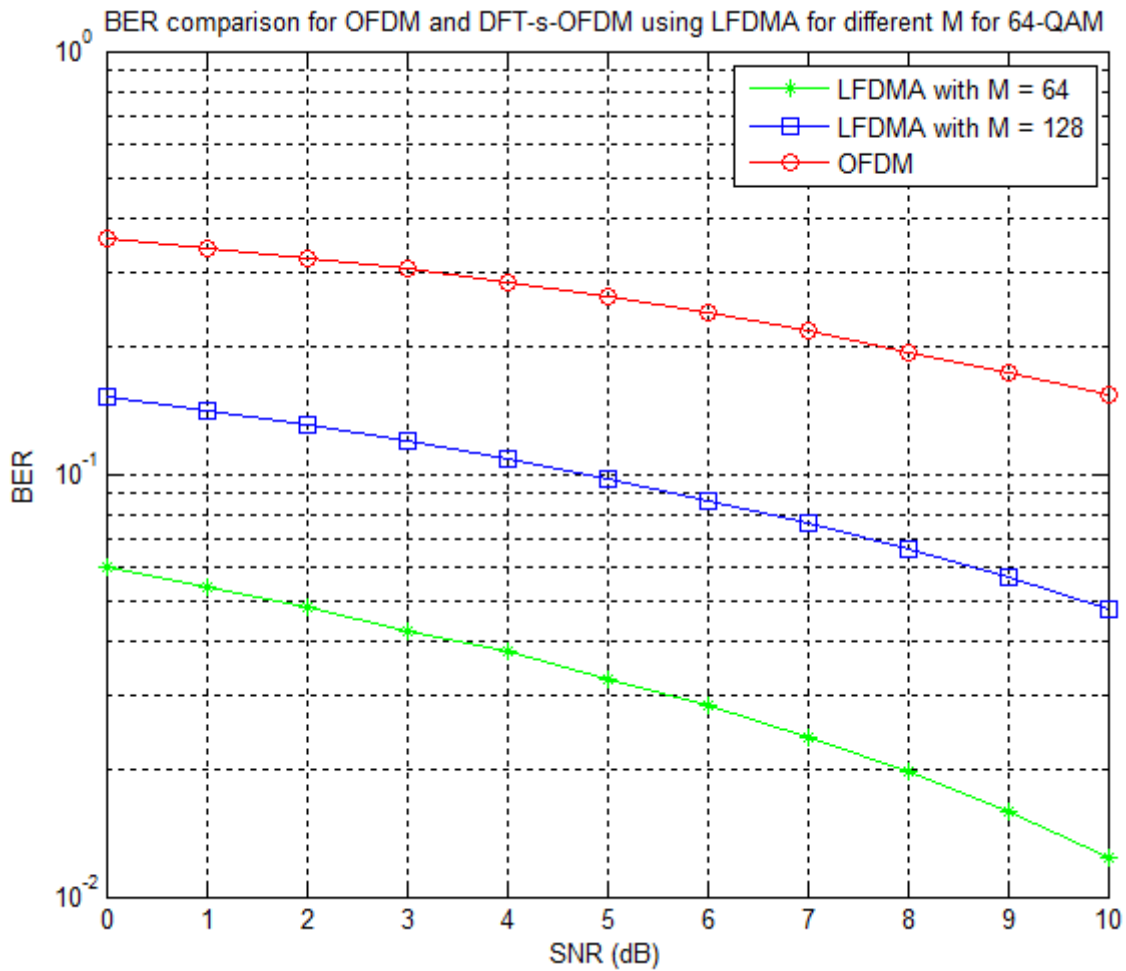


Fig. 5.8 : BER comparison of LFDMA and OFDM for 64-QAM

Similarly DFDMA and IFDMA have been simulated for M = 64 and M = 128. The plots for different modulation schemes for both cases are plotted in Fig. 5.9 and Fig. 5.10

The plot shown in Fig. 5.9 compares the BER v/s SNR for different spreading techniques when different modulation techniques have been used when $M = 64$

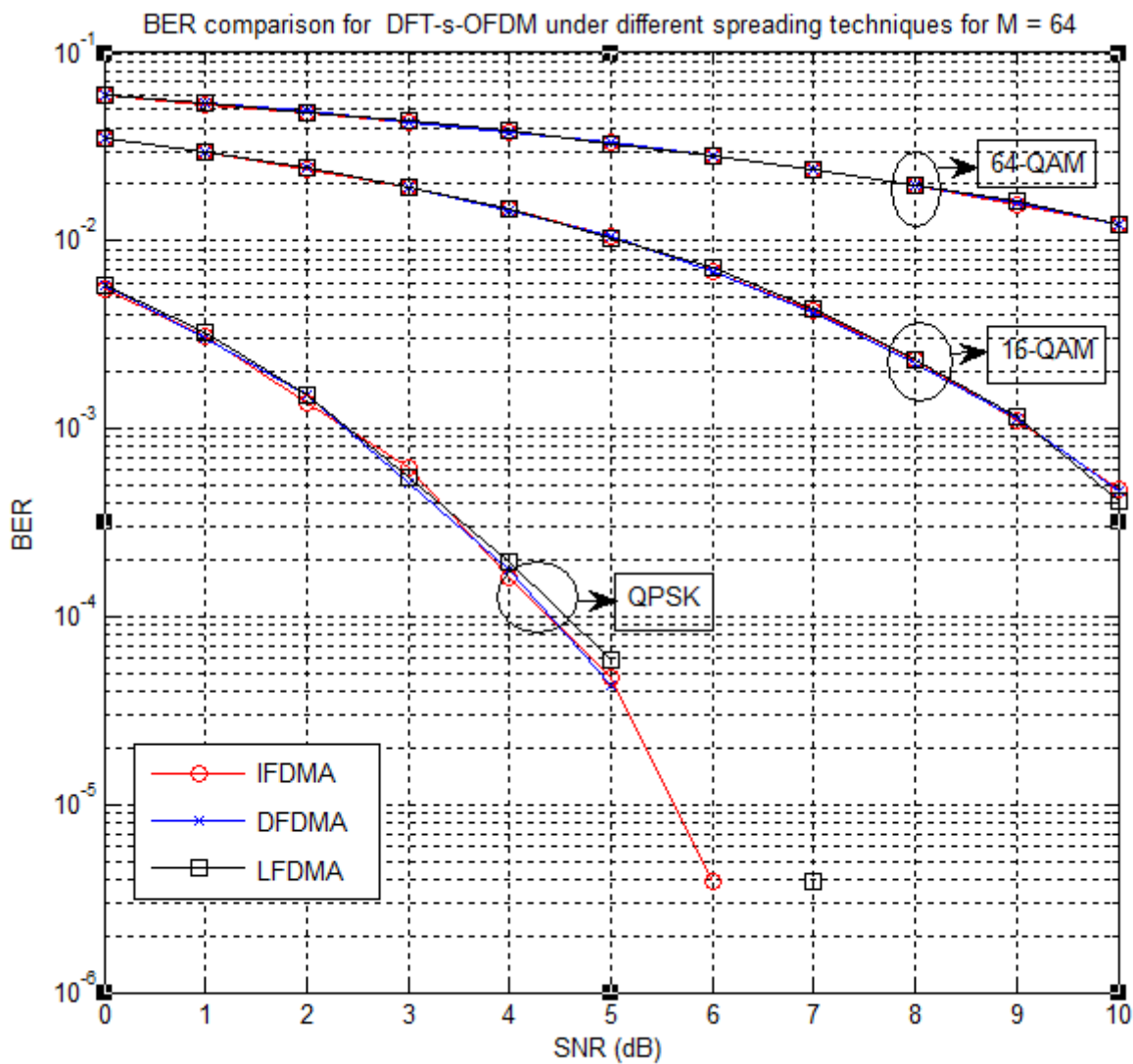


Fig. 5.9 : BER comparison of different spreading technique($M = 64$)

For QPSK modulation IFDMA and DFDMA have slightly better performance than LFDMA technique. For QAM modulation the performance is almost same.

The plot shown in Fig. 5.9 compares the BER v/s SNR for different spreading techniques when different modulation techniques have been used when $M = 128$

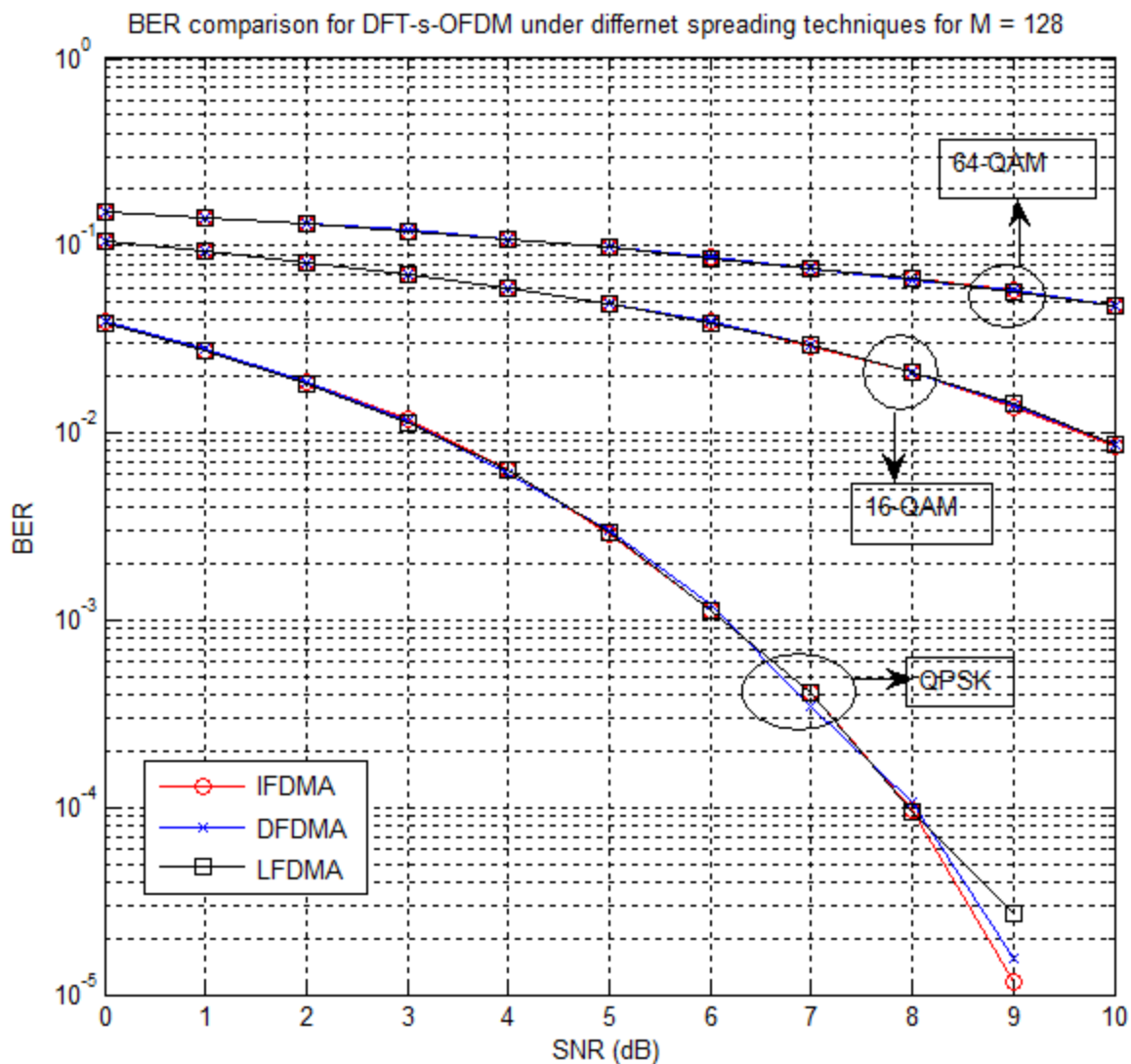


Fig. 5.10 : BER comparison for $M = 128$

It is evident from the plots that all the three spreading techniques have identical performance. These simulations were for the case when DFT has been used for spreading. The following section illustrates the use of DCT and DST as transform for spreading the signal.

5.3 SIMULATION RESULTS FOR DCT AND DST SPREADING

The simulation model for DCT and DST is same for DFT-s-OFDM except the M-point FFT and IFFT blocks are replaced by DCT and DST and analysis is done for M = 64 case.

5.3.1 Simulation results for IFDMA

In the Fig. 5.11 in case of QPSK DST has better performance and all have approximately same performance for QAM techniques

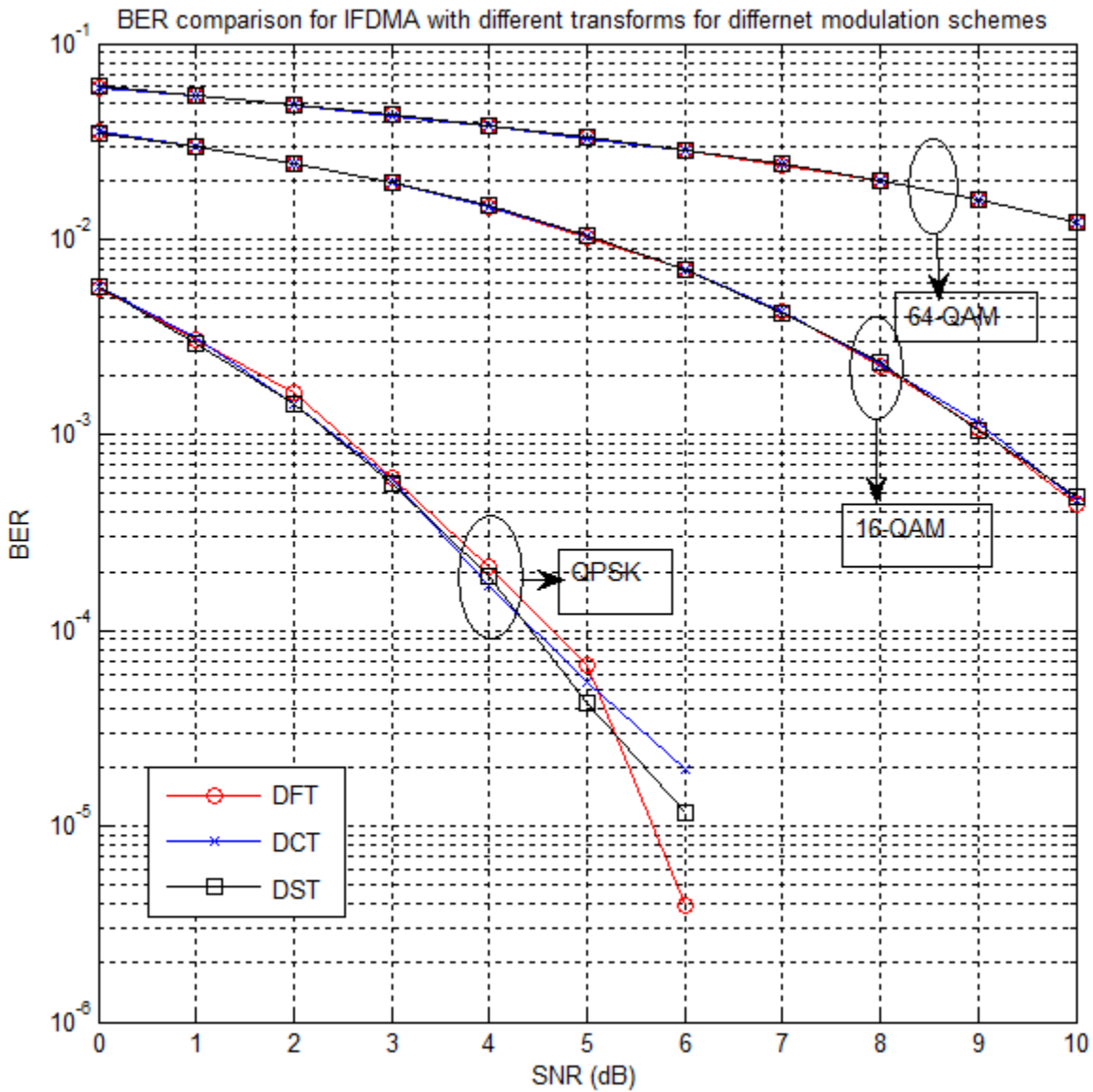


Fig. 5.11 : BER comparison for IFDMA

5.3.2 Simulation results for DFDMA

In the Fig. 5.12 in case of QPSK DST has better performance. For the case of 16-QAM DCT has the worst performance and for 64-QAM performance is almost same

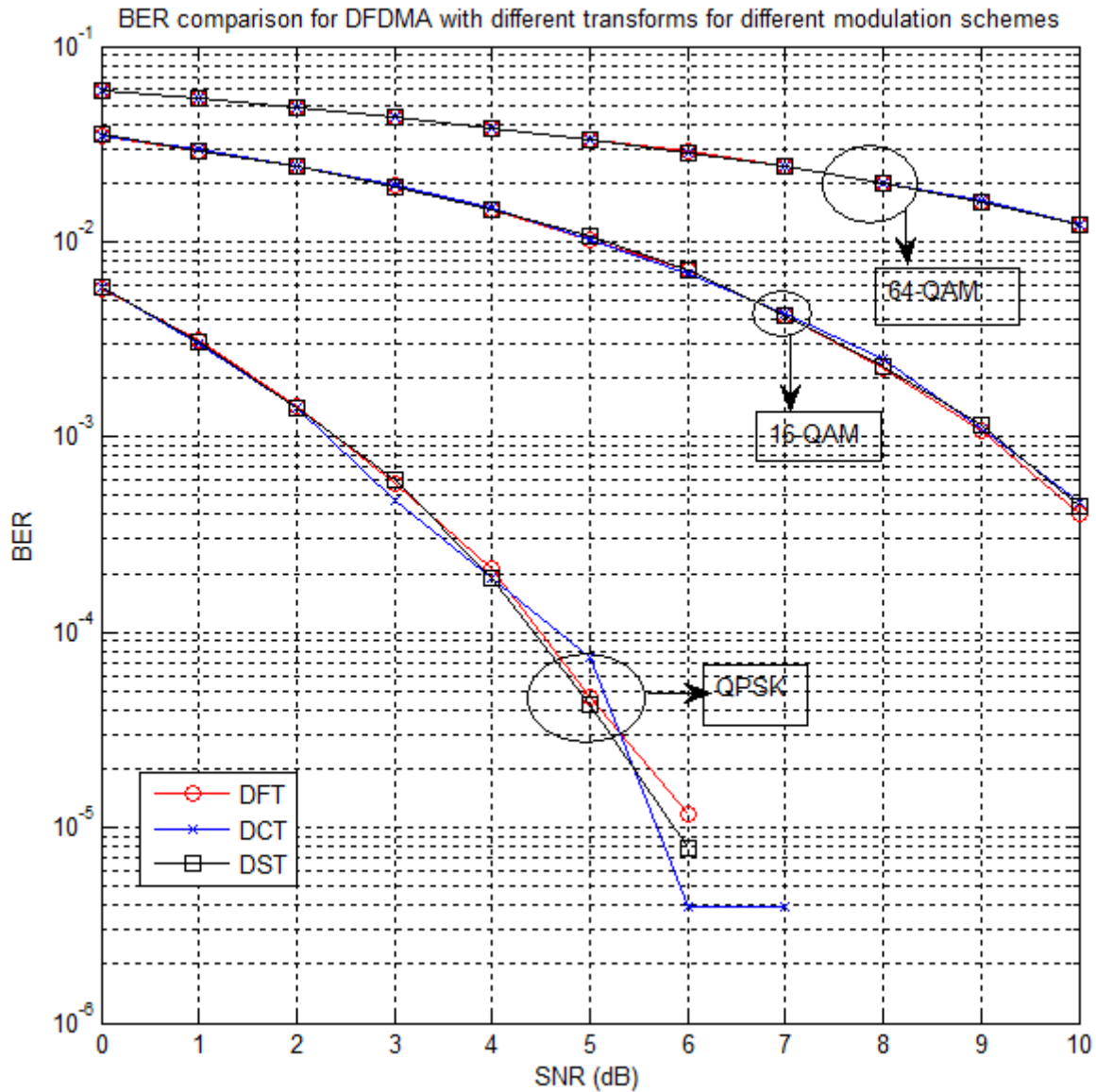


Fig. 5.12 : BER comparison for DFDMA

5.3.3 Simulation results for LFDMA

In the Fig.5.13 in case of QPSK DCT has better performance. For the case of 16-QAM DFT has the best performance and for 64-QAM performance is almost same

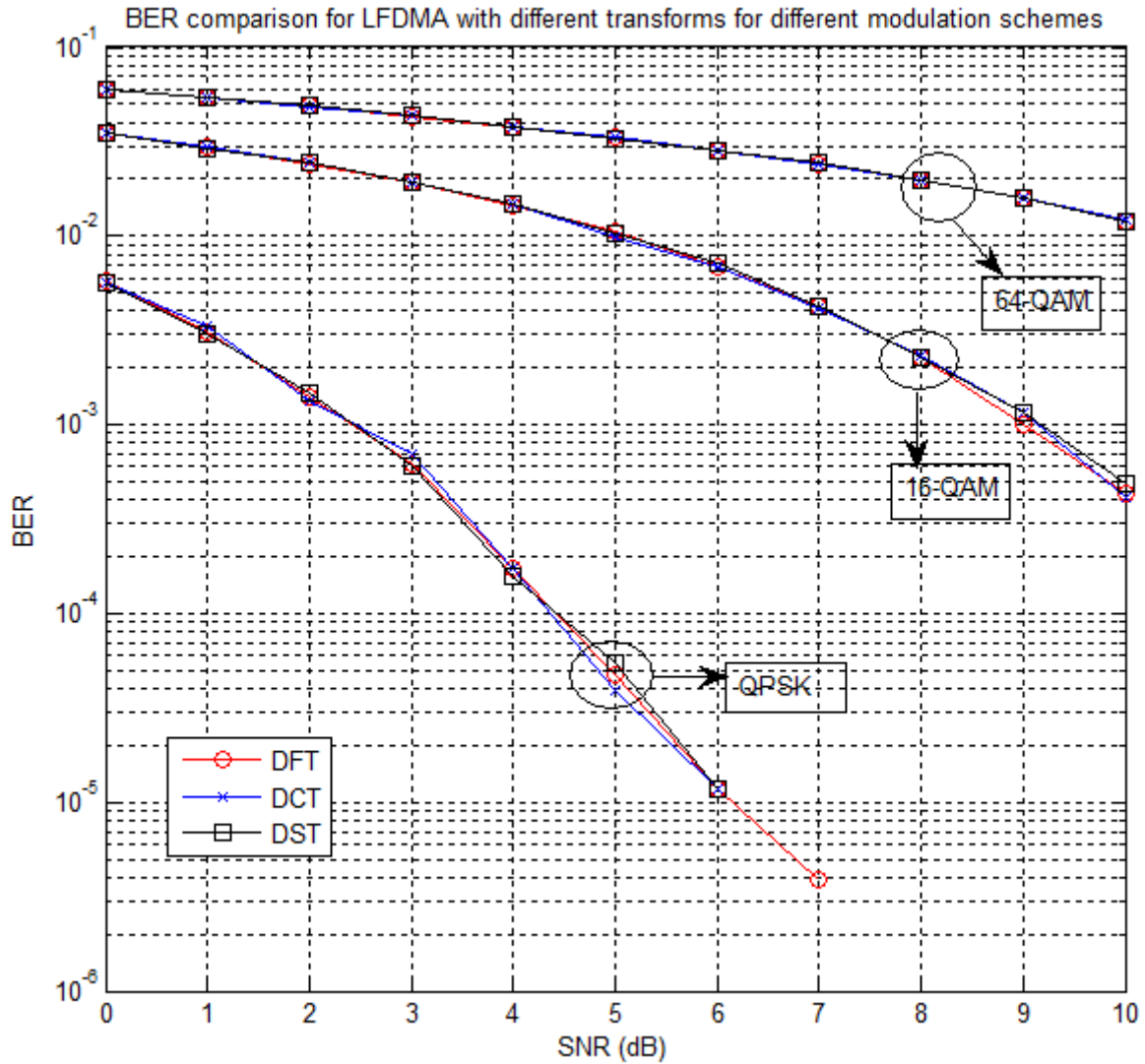


Fig. 5.13 : BER comparison for LFDMA

Thus, the use of DCT and DST as transform has better or comparable result and thus, can be used alternatively instead of DFT/FFT.

5.5 SIMULATIONS FOR PAPR ANALYSIS

As shown in Fig. 5.1 and 5.3 the PAPR calculation is done on the output of IFFT block. The PAPR performance is plotted as CCDF v/s PAPR, which gives the probability for different values of PAPR. As shown in previous chapters the PAPR of OFDM system is linearly dependent on number of sub-carriers. This has been simulated for QPSK modulation as in Fig. 5.14

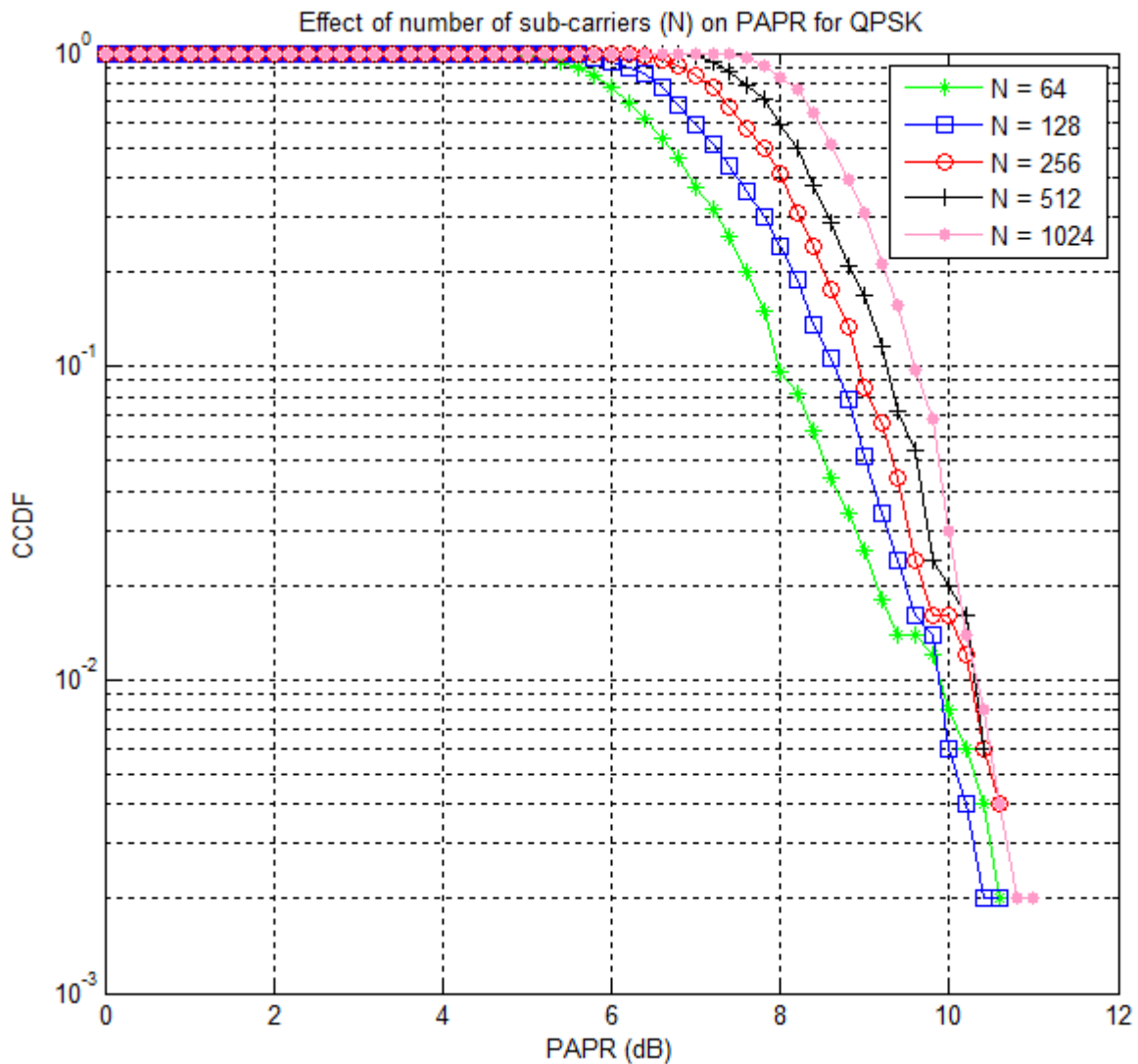


Fig. 5.14: Effect of N on PAPR

5.5.2 PAPR performance for 16-QAM

For the case of QPSK, IFDMA also gives the best performance as in seen in Fig. 5.16. The PAPR is 3.2 dB, 7.4 dB, 7.8 dB and 9.8 dB with 1.16% probability for IFDMA, LFDMA, DFDMA and OFDM respectively.

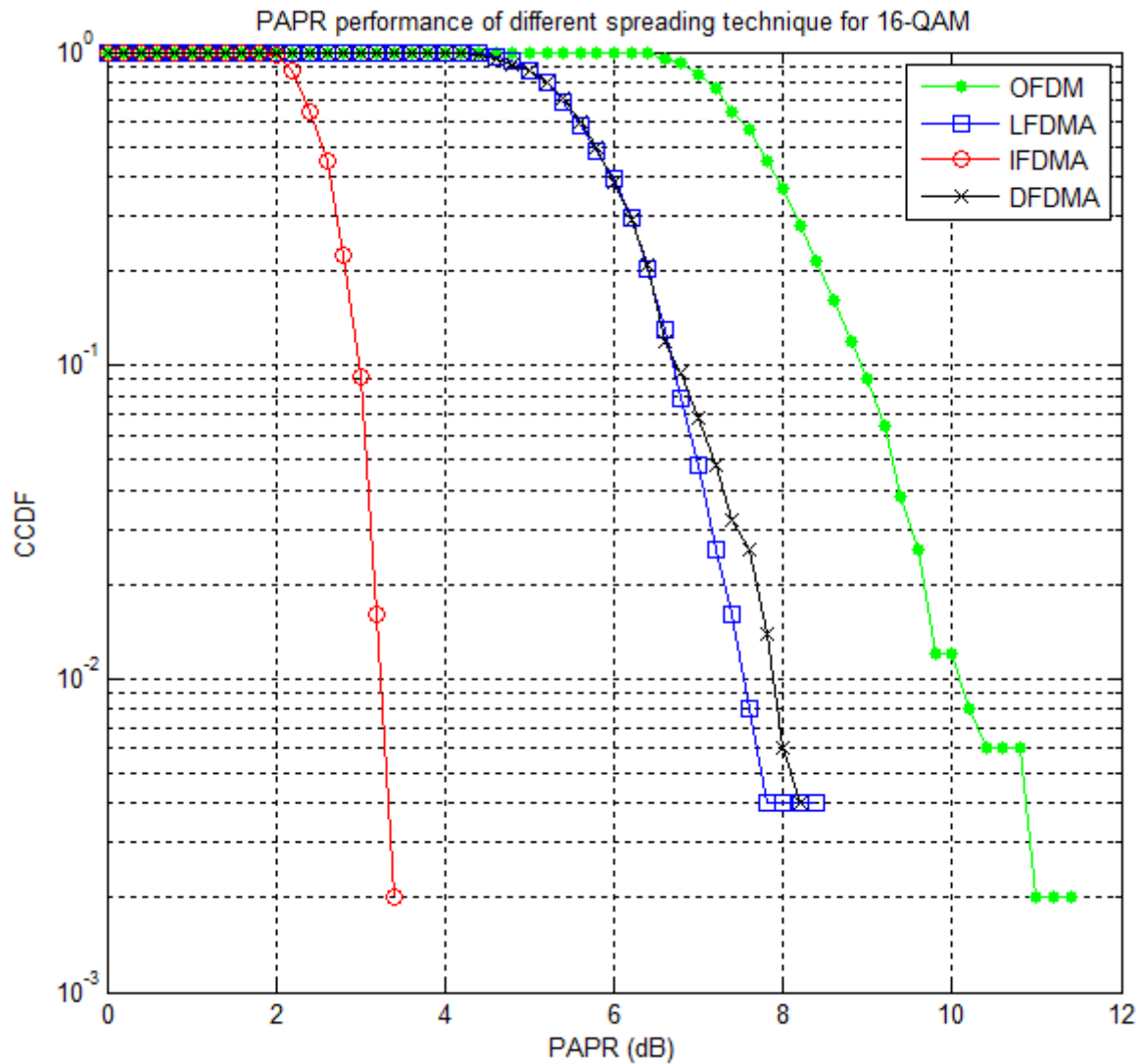


Fig. 5.16 : PAPR performance in 16-QAM

5.5.3 PAPR performance for 64-QAM

In the case 64-QAM, IFDMA gives the best performance. Thus, IFDMA is the best spreading algorithm from IFDMA, DFDMA and LFDMA

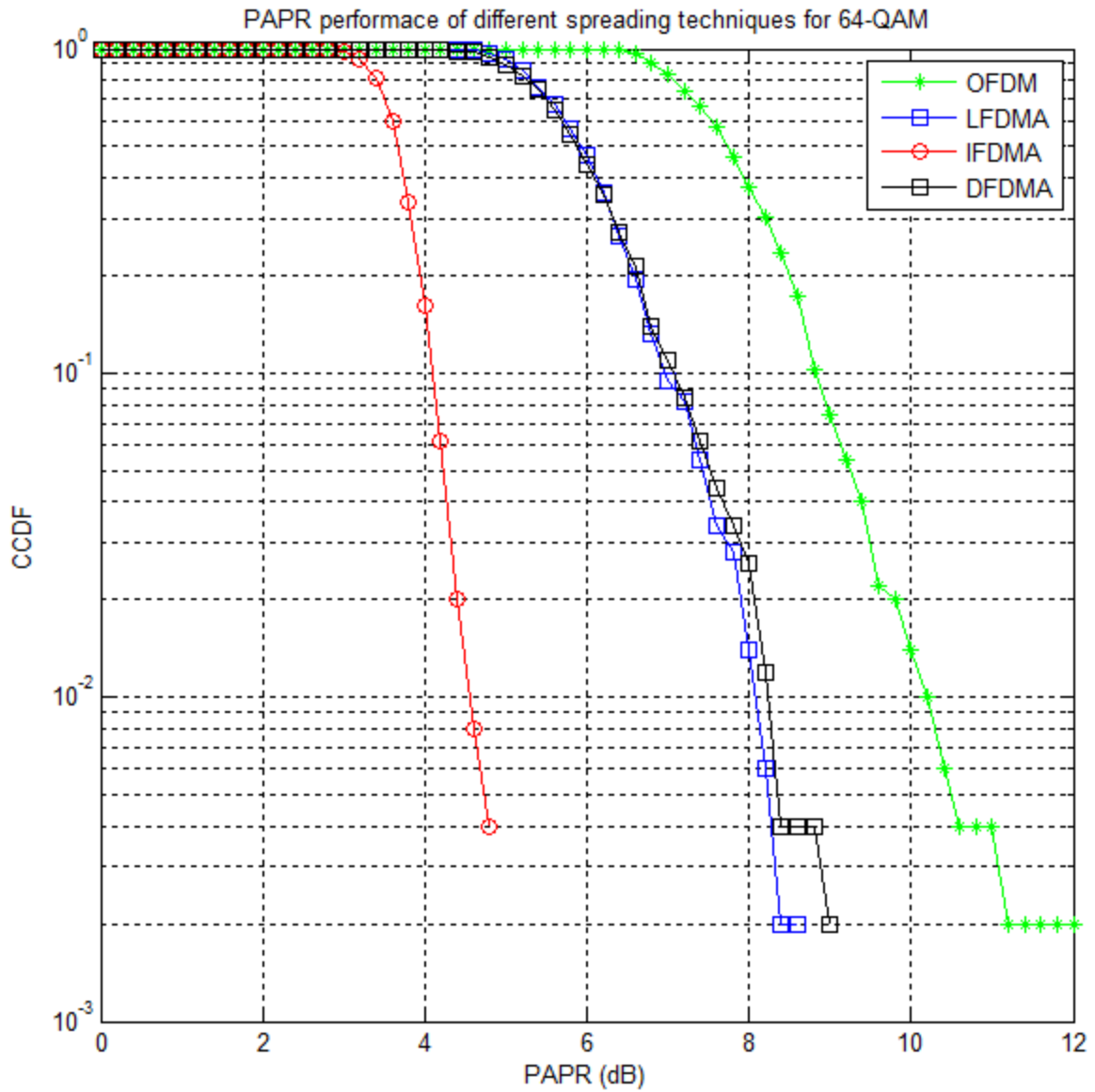


Fig. 5.16 : PAPR performance in 64-QAM

5.5.4 PAPR performance for different transforms for LFDMA

The performance for spreading by DFT is better than DCT and DST as in Fig. 5.18. The performance of DCT and DST is almost identical and much better than OFDM.

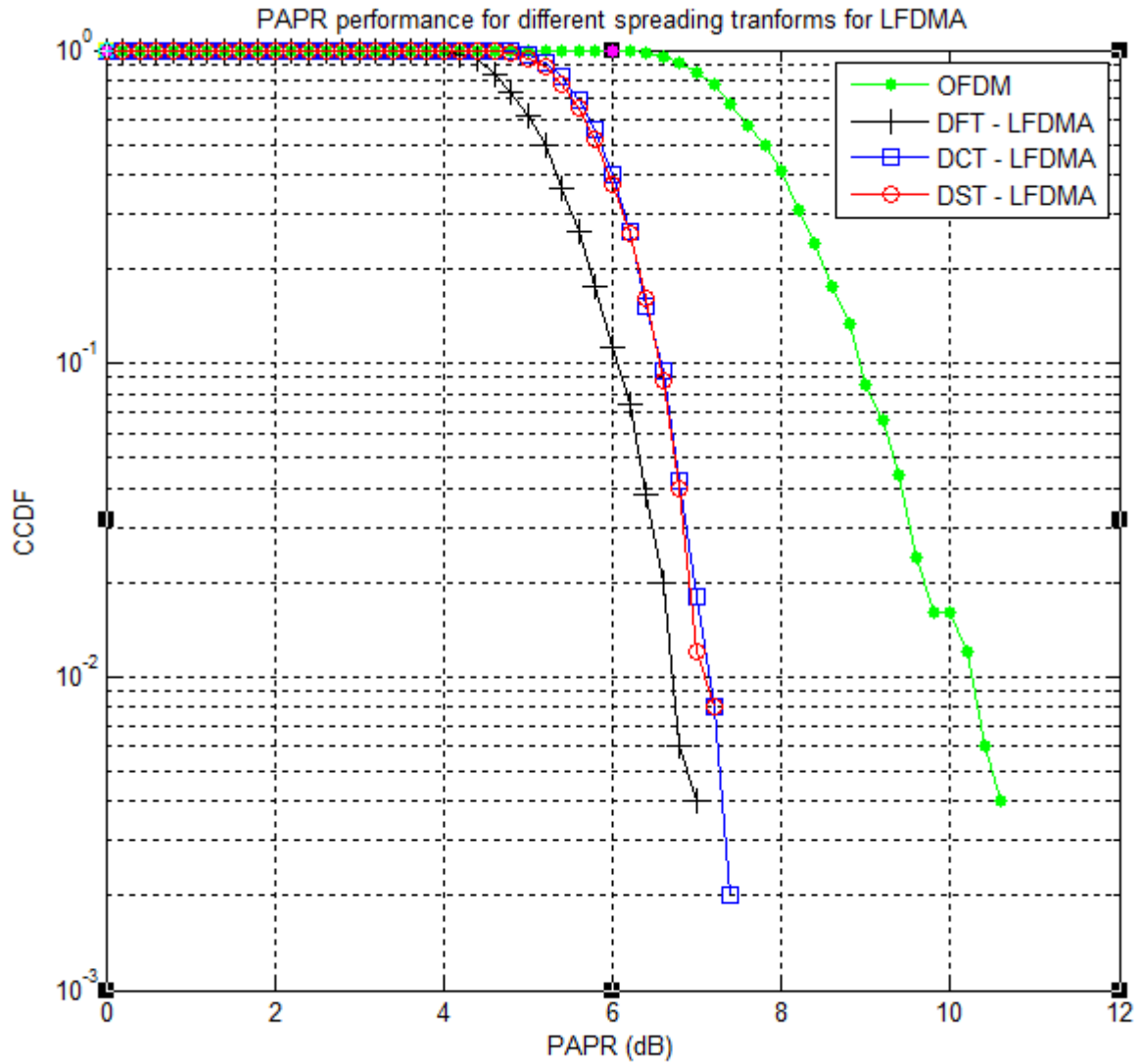


Fig. 5.18: PAPR performance of different transforms in LFDMA

5.5.5 PAPR performance for different transforms for DFDMA

The performance for spreading by is almost comparable as in Fig. 5.19 and all have better PAPR than OFDM

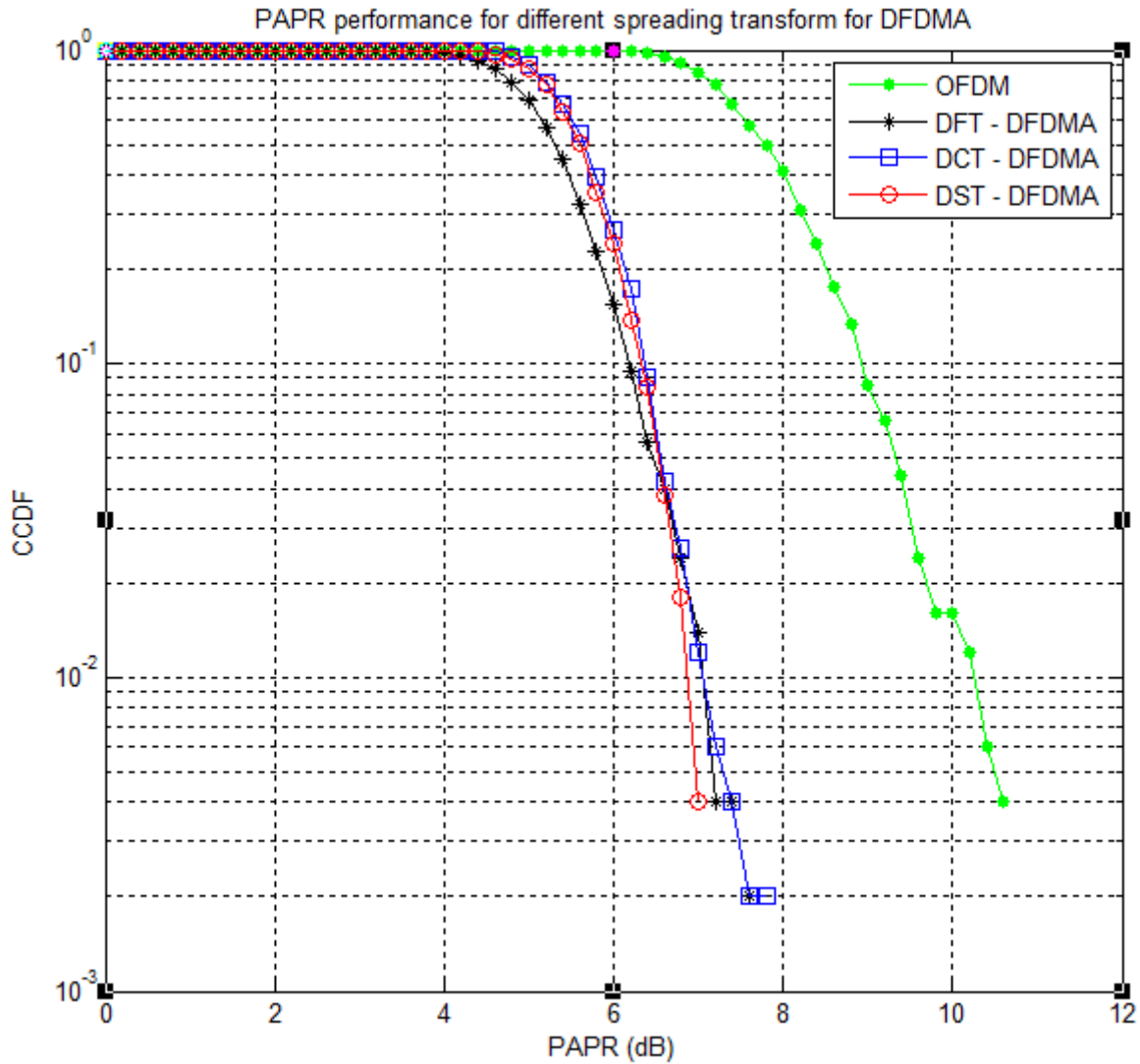


Fig. 5.19: PAPR performance of different transforms in DFDMA

5.5.6 PAPR performance for different transforms for IFDMA

The performance for spreading by DFT is far better than DCT and DST as in Fig. 5.20. The performance of DCT and DST is almost identical and much better than OFDM.

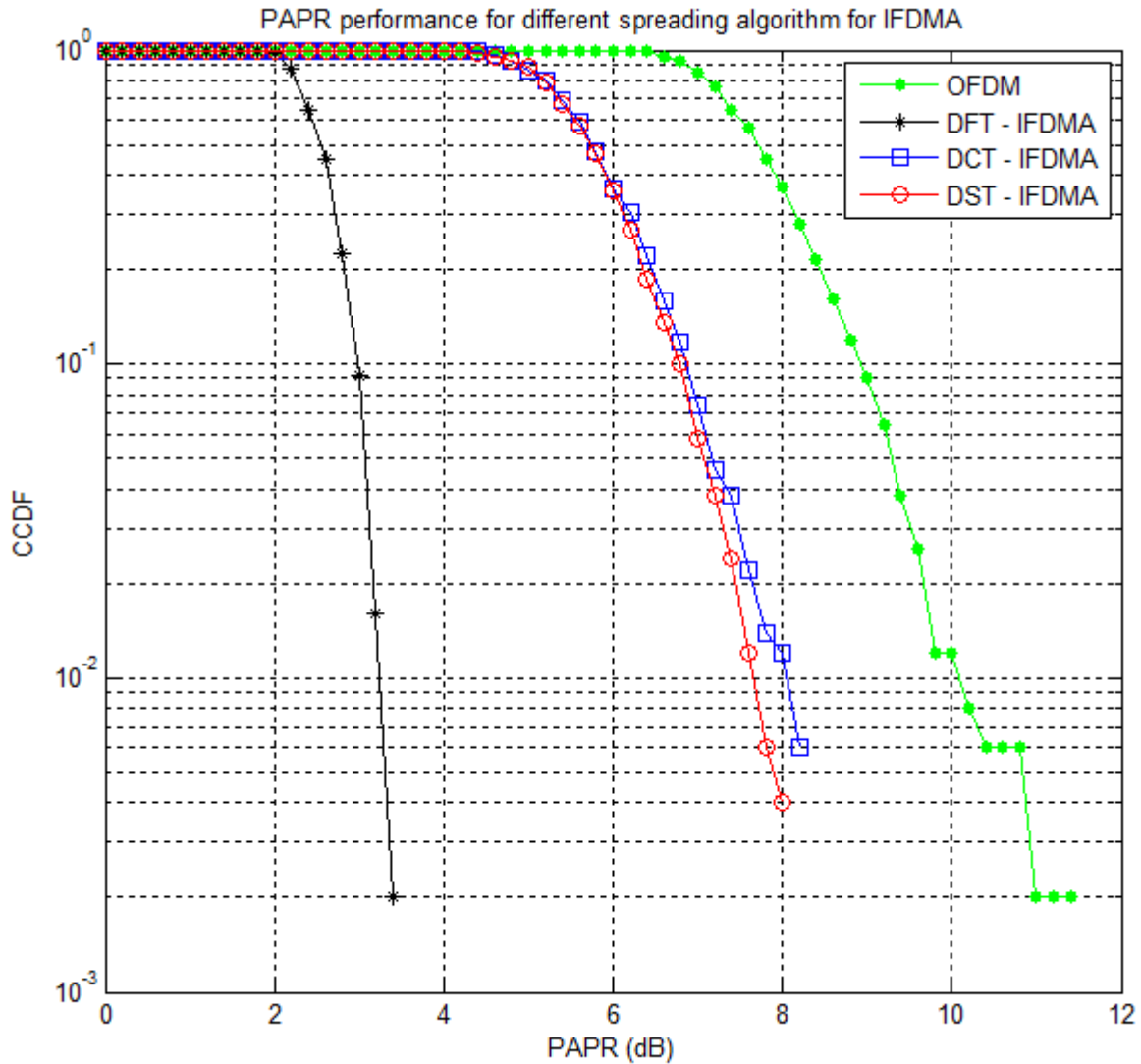


Fig. 5.18: PAPR performance of different transforms in LFDMA

The use of DCT and DST can be used as an alternative to DFT as BER and PAPR performance is almost identical and in some cases superior than DFT. The advantage of these transforms is that these are real transform and thus, hardware realization is easier for real arithmetic

CHAPTER 6

CONCLUSION AND FUTURE WORK

The models for both OFDM and SC-FDMA system for AWGN channel have been simulated. The simulation has been done for the case of QPSK, 16-QAM and 64-QAM modulation schemes. The spreading has been done using DFT, DCT and DST. The performance of these systems has been measured in terms of BER and PAPR. Analyzing the plots it can be concluded that even if spreading is done by DST or DCT there is a reduction in PAPR with respect to OFDM. Although DFT spreading has the lowest PAPR in all the three cases of LFDMA, DFDMA and IFDMA, but the values for DST and DCT are not very high. Also the BER performance is same in case of DFT, DCT and DST. Hence, these are good alternatives for DFT for the spreading of symbol energy. Thus, DCT and DST can be used as there is no severe performance degradation in BER and PAPR from DFT and in some cases the performance is better.

These DCT-s-OFDM and DST-s-OFDM schemes can be further modified by combining them with techniques to reduce ISI or negate the effects of CFO. The simulations have been done for AWGN channel and this work can be further extended for the case of ISI channels and similarly DCT and DST can be used instead of DFT in existing techniques to reduce the effect of ISI.

The OFDM and SC-FDMA model simulated can also be implemented on the Software Defined Radio (SDR). A SDR is an effective way to test a communication system without actually building the communication system. These systems can simulated on the SDR and can be tested for real signals like speech signals and text messages

APPENDIX 1

MATLAB CODE FOR BER AND PAPR SIMULATION

```
%% This is the main function where other functions have been called and -
simulation have been plotted
SNR = 0:10; % Range of Signal to Noise Ratio
Nbps = [2 4 6];%2/4/6 for QPSK/16-QAM/64-QAM respectively
dBs = 0:0.2:12;
%% BASIC OFDM
[BER_ofdm_QPSK,CCDF_ofdm_QPSK] = OFDM2(256,2,SNR); %Simulation of OFDM for
QPSK

% Calculation of CCDF to see the effect of N on PAPR
[~,CCDF_ofdm_QPSK_64] = OFDM(64,2,SNR);
[~,CCDF_ofdm_QPSK_128] = OFDM(128,2,SNR);
[~,CCDF_ofdm_QPSK_512] = OFDM(512,2,SNR);
[~,CCDF_ofdm_QPSK_1024] = OFDM(1024,2,SNR);

[BER_ofdm_16QAM,CCDF_ofdm_16QAM] = OFDM(256,4,SNR); %Simulation of OFDM for
16-QAM
[BER_ofdm_64QAM,CCDF_ofdm_64QAM] = OFDM(256,6,SNR); %Simulation of OFDM for
64-QAM

%% LOCALIZED FREQUENCY DIVISION MULTIPLEXING WITH DFT for M = 64 and M =
128

[BER_LFDMA_64,CCDF_LFDMA_64] = LFDMA(256,64,Nbps,SNR);
[BER_LFDMA_128,CCDF_LFDMA_128] = LFDMA(256,128,Nbps,SNR);

%% INTERLEAVED FREQUENCY DIVISION MULTIPLEXING WITH DFT for M = 64 and M =
128
[BER_IFDMA_64,CCDF_IFDMA_64] = IFDMA(256,64,Nbps,SNR);
[BER_IFDMA_128,CCDF_IFDMA_128] = IFDMA(256,128,Nbps,SNR);

%% DISTRIBUTED FREQUENCY DIVISION MULTIPLEXING WITH DFT for M = 64 and M =
128
[BER_DFDMA_64,CCDF_DFDMA_64] = DFDMA(256,64,Nbps,SNR);
[BER_DFDMA_128,CCDF_DFDMA_128] = DFDMA(256,128,Nbps,SNR);

%% SPREADING USING DCT for M = 64
[BER_LFDMA_64_DCT,CCDF_LFDMA_64_DCT] = LFDMADCT(256,64,Nbps,SNR);
[BER_IFDMA_64_DCT,CCDF_IFDMA_64_DCT] = IFDMADCT(256,64,Nbps,SNR);
[BER_DFDMA_64_DCT,CCDF_DFDMA_64_DCT] = DFDMADCT(256,64,Nbps,SNR);

%% SPREADING USING DST for M = 64
[BER_LFDMA_64_DST,CCDF_LFDMA_64_DST] = LFDMADST(256,64,Nbps,SNR);
[BER_IFDMA_64_DST,CCDF_IFDMA_64_DST] = IFDMADST(256,64,Nbps,SNR);
[BER_DFDMA_64_DST,CCDF_DFDMA_64_DST] = DFDMADST(256,64,Nbps,SNR);

%%PLOTS FOR BER COMPARISON
```

```

%% This plots the BER comparison for QPSK for OFDM and LFDMA
figure(1)
semilogy(SNR,BER_LFDMA_64(1,:), '-*g',SNR,BER_LFDMA_128(1,:), '-
s',SNR,BER_ofdm_QPSK, '-or');
legend('LFDMA with M = 64','LFDMA with M = 128','OFDM'); grid on;

%% This plots the BER comparison for 16-QAM for OFDM and LFDMA
figure(2)
semilogy(SNR,BER_LFDMA_64(2,:), '-*g',SNR,BER_LFDMA_128(2,:), '-
s',SNR,BER_ofdm_16QAM, '-or');
legend('LFDMA with M = 64','LFDMA with M = 128','OFDM'); grid on;

%% This plots the BER comparison for 64-QAM for OFDM and LFDMA
figure(3)
semilogy(SNR,BER_LFDMA_64(3,:), '-*g',SNR,BER_LFDMA_128(3,:), '-
s',SNR,BER_ofdm_64QAM, '-or');
legend('LFDMA with M = 64','LFDMA with M = 128','OFDM'); grid on;

%% This plots the BER results for IDFDMA, LFDMA and DFDM for all modulation
schemes for M = 64
figure(4)
semilogy(SNR,BER_IDFDMA_64(1,:), '-or',SNR,BER_DFDM_64(1,:), '-
xb',SNR,BER_LFDMA_64(1,:), '-sk');
legend('IDFDMA','DFDM','LFDMA'); grid on;
hold on;

semilogy(SNR,BER_IDFDMA_64(2,:), '-or',SNR,BER_DFDM_64(2,:), '-
xb',SNR,BER_LFDMA_64(2,:), '-sk');
legend('IDFDMA','DFDM','LFDMA'); grid on;
hold on;

semilogy(SNR,BER_IDFDMA_64(3,:), '-or',SNR,BER_DFDM_64(3,:), '-
xb',SNR,BER_LFDMA_64(3,:), '-sk');
legend('IDFDMA','DFDM','LFDMA'); grid on;
hold on;

%% This plots the BER results for IDFDMA, LFDMA and DFDM for all modulation
schemes for M = 128
figure(4)
semilogy(SNR,BER_IDFDMA_128(1,:), '-or',SNR,BER_DFDM_128(1,:), '-
xb',SNR,BER_LFDMA_128(1,:), '-sk');
legend('IDFDMA','DFDM','LFDMA'); grid on;
hold on;

semilogy(SNR,BER_IDFDMA_128(2,:), '-or',SNR,BER_DFDM_128(2,:), '-
xb',SNR,BER_LFDMA_128(2,:), '-sk');
legend('IDFDMA','DFDM','LFDMA'); grid on;
hold on;

semilogy(SNR,BER_IDFDMA_128(3,:), '-or',SNR,BER_DFDM_128(3,:), '-
xb',SNR,BER_LFDMA_128(3,:), '-sk');
legend('IDFDMA','DFDM','LFDMA'); grid on;
hold on;

```

```

%% This plots the BER results for IFDMA for all modulation for all transform
spreading for M = 64
figure(5)
semilogy(SNR,BER_IFDMA_64(1,:), '-or',SNR,BER_IFDMA_64_DCT(1,:), '-
xb',SNR,BER_IFDMA_64_DST(1,:), '-sk');
legend('DFT','DCT','DST'); grid on;
hold on;

semilogy(SNR,BER_IFDMA_64(2,:), '-or',SNR,BER_IFDMA_64_DCT(2,:), '-
xb',SNR,BER_IFDMA_64_DST(2,:), '-sk');
legend('DFT','DCT','DST'); grid on;
hold on;

semilogy(SNR,BER_IFDMA_64(3,:), '-or',SNR,BER_IFDMA_64_DCT(3,:), '-
xb',SNR,BER_IFDMA_64_DST(3,:), '-sk');
legend('DFT','DCT','DST'); grid on;
hold on;

%% This plots the BER results for DFDMA for all modulation for all
transform spreading for M = 64
figure(6)
semilogy(SNR,BER_DFDMA_64(1,:), '-or',SNR,BER_DFDMA_64_DCT(1,:), '-
xb',SNR,BER_DFDMA_64_DST(1,:), '-sk');
legend('DFT','DCT','DST'); grid on;
hold on;

semilogy(SNR,BER_DFDMA_64(2,:), '-or',SNR,BER_DFDMA_64_DCT(2,:), '-
xb',SNR,BER_DFDMA_64_DST(2,:), '-sk');
legend('DFT','DCT','DST'); grid on;
hold on;

semilogy(SNR,BER_DFDMA_64(3,:), '-or',SNR,BER_DFDMA_64_DCT(3,:), '-
xb',SNR,BER_DFDMA_64_DST(3,:), '-sk');
legend('DFT','DCT','DST'); grid on;
hold on;

%% This plots the BER results for LFDMA for all modulation for all
transform spreading for M = 64
figure(7)
semilogy(SNR,BER_LFDMA_64(1,:), '-or',SNR,BER_LFDMA_64_DCT(1,:), '-
xb',SNR,BER_LFDMA_64_DST(1,:), '-sk');
legend('DFT','DCT','DST'); grid on;
hold on;

semilogy(SNR,BER_LFDMA_64(2,:), '-or',SNR,BER_LFDMA_64_DCT(2,:), '-
xb',SNR,BER_LFDMA_64_DST(2,:), '-sk');
legend('DFT','DCT','DST'); grid on;
hold on;

semilogy(SNR,BER_LFDMA_64(3,:), '-or',SNR,BER_LFDMA_64_DCT(3,:), '-
xb',SNR,BER_LFDMA_64_DST(3,:), '-sk');
legend('DFT','DCT','DST'); grid on;
hold on;

```

```

%% PLOTS FOR CCDF COMPARISON

%% This plots the effect of increasing N on PAPR for QPSK
figure(8);
semilogy(dBs,CCDF_ofdm_QPSK_64,'-*g',dBs,CCDF_ofdm_QPSK_128,'-
s',dBs,CCDF_ofdm_QPSK,'-or',dBs,CCDF_ofdm_QPSK_512,'-
b',dBs,CCDF_ofdm_QPSK_1024,'-c');
legend('N = 64','N = 128','N = 256','N = 512','N = 1024'); grid on;

%% This plots the PAPR performance of different spreading algorithms for
QPSK
figure(9)
semilogy(dBs,CCDF_ofdm_QPSK,'-*g',dBs,CCDF_LFDMA_64(1,:),'-
s',dBs,CCDF_IFDMA_64(1,:),'-or',dBs,CCDF_DFDMA_64(1,:),'-sk');
legend('OFDM','LFDMA','IFDMA','DFDMA'); grid on;

%% This plots the PAPR performance of different spreading algorithms for
16-QAM
figure(10)
semilogy(dBs,CCDF_ofdm_16QAM,'-*g',dBs,CCDF_LFDMA_64(2,:),'-
s',dBs,CCDF_IFDMA_64(2,:),'-or',dBs,CCDF_DFDMA_64(2,:),'-sk');
legend('OFDM','LFDMA','IFDMA','DFDMA'); grid on;

%% This plots the PAPR performance of different spreading algorithms for
64-QAM
figure(11)
semilogy(dBs,CCDF_ofdm_64QAM,'-*g',dBs,CCDF_LFDMA_64(3,:),'-
s',dBs,CCDF_IFDMA_64(3,:),'-or',dBs,CCDF_DFDMA_64(3,:),'-sk');
legend('OFDM','LFDMA','IFDMA','DFDMA'); grid on;

%% This plots the PAPR performance for different spreading transforms for
LFDMA
figure(12)
semilogy(dBs,CCDF_ofdm_QPSK,'-*g',dBs,CCDF_LFDMA_64(1,:),'-
*g',dBs,CCDF_LFDMA_64_DCT(1,:),'-s',dBs,CCDF_LFDMA_64_DST(1,:),'-or');
legend('OFDM','DFT - LFDMA','DCT - LFDMA','DST - LFDMA'); grid on;

%% This plots the PAPR performance for different spreading transforms for
DFDMA
figure(13)
semilogy(dBs,CCDF_ofdm_QPSK,'-*g',dBs,CCDF_DFDMA_64(1,:),'-
*g',dBs,CCDF_DFDMA_64_DCT(1,:),'-s',dBs,CCDF_DFDMA_64_DST(1,:),'-or');
legend('OFDM','DFT - DFDMA','DCT - DFDMA','DST - DFDMA'); grid on;

%% This plots the PAPR performance for different spreading transforms for
IFDMA
figure(14)
semilogy(dBs,CCDF_ofdm_16QAM,'-*g',dBs,CCDF_IFDMA_64(2,:),'-
*g',dBs,CCDF_IFDMA_64_DCT(2,:),'-s',dBs,CCDF_IFDMA_64_DST(2,:),'-or');
legend('OFDM','DFT - IFDMA','DCT - IFDMA','DST - IFDMA'); grid on;

```

```

%% This function simulates the OFDM scheme for AWGN channel
function [BER,CCDF] = OFDM(Nfft,Nbps,SNR)
%% This function simulates the OFDM scheme for AWGN channel
M=2^Nbps; % Modulation order=2/4/6 for QPSK/16QAM/64QAM
Nframe = 500;
Berebn0 = zeros(1,Nframe);
Ber = zeros(1,length(SNR));
norms=[1 sqrt(2) 0 sqrt(10) 0 sqrt(42)]; % BPSK 4-QAM/QPSK 16-QAM 64-
QAM
PAPR = zeros(1,Nframe);
for i = 1:length(SNR)
    for j = 1:Nframe
        Neb = 0;
        X= (randi(M,1,Nfft) - 1); % Generation of random data
        Xmod= qammod(X,M,0,'gray')/norms(Nbps); % Modulation
        X_ifft = ifft(Xmod,Nfft); % N-point IFFT
        if (i == 1) % PAPR calculation
            sym_pow = X_ifft.*conj(X_ifft); % measure symbol power
            PAPR(j) = max(sym_pow)/mean(sym_pow); % measure PAPR
        end
        X_GI = [X_ifft((Nfft - Nfft/4) + 1):Nfft) X_ifft]; % Addition
of CP
        y_GI = awgn(X_GI,SNR(i),'measured'); %Addition of noise
        y = y_GI((Nfft/4)+1):(Nfft + Nfft/4)); %Removal of CO
        Y = fft(y,Nfft); %N-point FFT
        X_r=qamdemod(Y*norms(Nbps),M,0,'gray'); %Demodulation
        Neb=Neb+sum(sum(de2bi(X_r,Nbps) ~= de2bi(X,Nbps))); % Error
Detecton
        Berebn0(j) = Neb/(Nfft*Nbps);
    end
    Ber(i) = mean(Berebn0); %Calculation of BER
end
BER = Ber;
CCDF = CCDF_calculation(PAPR,Nframe); % Calculation of CCDF
end

%% This function simulates the LFDMA scheme for AWGN channel for DFT
function [BER,CCDF] = LFDMA(Nfft,Nfdma,N,SNR)
Nframe = 500;
Berebn0 = zeros(1,Nframe);
Ber = zeros(length(N),length(SNR));
norms=[1 sqrt(2) 0 sqrt(10) 0 sqrt(42)]; % BPSK 4-QAM/QPSK 16-QAM 64-
QAM
PAPR = zeros(1,Nframe);
for index = 1:length(N)
    Nbps = N(index);
    M=2^Nbps; % Modulation order=2/4/6 for QPSK/16QAM/64QAM
    for i = 1:length(SNR)
        for j = 1:Nframe
            Neb = 0;
            X= (randi(M,1,Nfdma) - 1); % Row vector of the symbols to
be transmitted
            Xmod= qammod(X,M,0,'gray')/norms(Nbps); % M-ary QAM
modulation

```



```

X_fdma = [fft(Xmod,Nfdma) zeros(1,Nfft-Nfdma)];
X_ifft = ifft(X_fdma,Nfft);
if (i == 1)
    sym_pow = X_ifft.*conj(X_ifft); % measure symbol power
    PAPR(j) = max(sym_pow)/mean(sym_pow); % measure PAPR
end
X_GI = [X_ifft(((Nfft - Nfft/4) + 1):Nfft) X_ifft];
y_GI = awgn(X_GI,SNR(i), 'measured');
y = y_GI(((Nfft/4)+1):(Nfft + Nfft/4));
Y = fft(y,Nfft);
Y_fdma = Y(1:Nfdma);
Y_fdma = ifft(Y_fdma,Nfdma);
X_r=qamdemod(Y_fdma*norms(Nbps),M,0,'gray');
Neb=Neb+sum(sum(de2bi(X_r,Nbps) ~= de2bi(X,Nbps)));
Berebn0(j) = Neb/(Nfft*Nbps);
end
Ber(index,i) = mean(Berebn0);
end
ccdf(index,:) = CCDF_calculation(PAPR,Nframe);
end
BER = Ber;
CCDF = ccdf;
end

```

% This function simulates the DFDMA scheme for AWGN channel using DFT

```

function [BER,CCDF] = DFDMA(Nfft,Nfdma,N,SNR)
Nframe = 500;
Berebn0 = zeros(1,Nframe);
Ber = zeros(length(N),length(SNR));
norms=[1 sqrt(2) 0 sqrt(10) 0 sqrt(42)]; % BPSK 4-QAM/QPSK 16-QAM 64-
QAM
X_ifdma = zeros(1,Nfft);
PAPR = zeros(1,Nframe);
for index = 1:length(N)
    Nbps = N(index);
    M=2^Nbps; % Modulation order=2/4/6 for QPSK/16QAM/64QAM
    for i = 1:length(SNR)
        for j = 1:Nframe
            Neb = 0;
            X= (randi(M,1,Nfdma) - 1); % Row vector of the symbols to
be transmitted
            Xmod= qammod(X,M,0,'gray')/norms(Nbps); % M-ary QAM
modulation
            X_fdma = fft(Xmod,Nfdma);
            X_ifdma(1:2:(2*Nfdma)) = X_fdma;
            X_ifft = ifft(X_ifdma,Nfft);
            if (i == 1)
                sym_pow = X_ifft.*conj(X_ifft); % measure symbol power
                PAPR(j) = max(sym_pow)/mean(sym_pow); % measure PAPR
            end
            X_GI = [X_ifft(((Nfft - Nfft/4) + 1):Nfft) X_ifft];
            y_GI = awgn(X_GI,SNR(i), 'measured');
            y = y_GI(((Nfft/4)+1):(Nfft + Nfft/4));
            Y = fft(y,Nfft);

```

```

        Y_fdma = Y(1:2:(2*Nfdma));
        Y_fdma = ifft(Y_fdma,Nfdma);
        X_r=qamdemod(Y_fdma*norms(Nbps),M,0,'gray');
        Neb=Neb+sum(sum(de2bi(X_r,Nbps) ~= de2bi(X,Nbps)));
        Berebn0(j) = Neb/(Nfft*Nbps);
    end
    Ber(index,i) = mean(Berebn0);
end
ccdf(index,:) = CCDF_calculation(PAPR,Nframe);
end
BER = Ber;
CCDF = ccdf;
end

%% This function simulates the OFDM scheme for AWGN channel using DFT
function [BER,CCDF] = IFDMA(Nfft,Nfdma,N,SNR)
    Nframe = 500;
    Berebn0 = zeros(1,Nframe);
    Ber = zeros(length(N),length(SNR));
    norms=[1 sqrt(2) 0 sqrt(10) 0 sqrt(42)]; % BPSK 4-QAM/QPSK 16-QAM 64-
QAM
    X_ifdma = zeros(1,Nfft);
    PAPR = zeros(1,Nframe);
    for index = 1:length(N)
        Nbps = N(index);
        M=2^Nbps; % Modulation order=2/4/6 for QPSK/16QAM/64QAM
        for i = 1:length(SNR)
            for j = 1:Nframe
                Neb = 0;
                X = (randi(M,1,Nfdma) - 1); % Row vector of the symbols to
be transmitted
                Xmod= qammod(X,M,0,'gray')/norms(Nbps); % M-ary QAM
modulation
                X_fdma = fft(Xmod,Nfdma);
                X_ifdma(1:(Nfft/Nfdma):end) = X_fdma;
                X_ifft = ifft(X_ifdma,Nfft);
                if (i == 1)
                    sym_pow = X_ifft.*conj(X_ifft); % measure symbol power
                    PAPR(j) = max(sym_pow)/mean(sym_pow); % measure PAPR
                end
                X_GI = [X_ifft(((Nfft - Nfft/4) + 1):Nfft) X_ifft];
                y_GI = awgn(X_GI,SNR(i),'measured');
                y = y_GI(((Nfft/4)+1):(Nfft + Nfft/4));
                Y = fft(y,Nfft);
                Y_fdma = Y(1:(Nfft/Nfdma):end);
                Y_fdma = ifft(Y_fdma,Nfdma);
                X_r=qamdemod(Y_fdma*norms(Nbps),M,0,'gray');
                Neb=Neb+sum(sum(de2bi(X_r,Nbps) ~= de2bi(X,Nbps)));
                Berebn0(j) = Neb/(Nfft*Nbps);
            end
            Ber(index,i) = mean(Berebn0);
        end
    end
    ccdf(index,:) = CCDF_calculation(PAPR,Nframe);
end
BER = Ber;

```

```

        CCDF = ccdf;
    end

function CCDF = CCDF_calculation(PAPR,Nframe)
%% This function calculates the CCDF for given PAPR values
    scale = 0:0.2:12;
    Hscale = scale+(scale(2)-scale(1))/2;
    PAPRscale = 10*log10(PAPR);
    N = hist(PAPRscale,Hscale);
    count = 0;
    for i=length(Hscale):-1:1
        count=count+N(i);
        CCDF(i)=count/Nframe;
    end
end

%% This function simulates the DFDMA scheme for AWGN channel using DCT
function [BER,CCDF] = DFDMA_DCT(Nfft,Nfdma,N,SNR)
    Nframe = 500;
    Berebn0 = zeros(1,Nframe);
    Ber = zeros(length(N),length(SNR));
    norms=[1 sqrt(2) 0 sqrt(10) 0 sqrt(42)]; % BPSK 4-QAM/QPSK 16-QAM 64-
QAM
    X_ifdma = zeros(1,Nfft);
    PAPR = zeros(1,Nframe);
    for index = 1:length(N)
        Nbps = N(index);
        M=2^Nbps; % Modulation order=2/4/6 for QPSK/16QAM/64QAM
        for i = 1:length(SNR)
            for j = 1:Nframe
                Neb = 0;
                X = (randi(M,1,Nfdma) - 1); % Row vector of the symbols to
be transmitted
                Xmod= qammod(X,M,0,'gray')/norms(Nbps); % M-ary QAM
modulation
                X_fdma = dct(Xmod,Nfdma);
                X_ifdma(1:2:(2*Nfdma)) = X_fdma;
                X_ifft = ifft(X_ifdma,Nfft);
                if (i == 1)
                    sym_pow = X_ifft.*conj(X_ifft); % measure symbol power
                    PAPR(j) = max(sym_pow)/mean(sym_pow); % measure PAPR
                end
                X_GI = [X_ifft(((Nfft - Nfft/4) + 1):Nfft) X_ifft];
                y_GI = awgn(X_GI,SNR(i),'measured');
                y = y_GI(((Nfft/4)+1):(Nfft + Nfft/4));
                Y = fft(y,Nfft);
                Y_fdma = Y(1:2:(2*Nfdma));
                Y_fdma = idct(Y_fdma,Nfdma);
                X_r=qamdemod(Y_fdma*norms(Nbps),M,0,'gray');
                Neb=Neb+sum(sum(de2bi(X_r,Nbps) ~= de2bi(X,Nbps)));
                Berebn0(j) = Neb/(Nfft*Nbps);
            end
            Ber(index,i) = mean(Berebn0);
        end
        ccdf(index,:) = CCDF_calculation(PAPR,Nframe);
    end
end

```

```

end
BER = Ber;
CCDF = ccdf;
end

%% This function simulates the DFDMA scheme for AWGN channel using DST
function [BER,CCDF] = DFDMA_DST(Nfft,Nfdma,N,SNR)
Nframe = 500;
Berebn0 = zeros(1,Nframe);
Ber = zeros(length(N),length(SNR));
norms=[1 sqrt(2) 0 sqrt(10) 0 sqrt(42)]; % BPSK 4-QAM/QPSK 16-QAM 64-
QAM
X_ifdma = zeros(1,Nfft);
PAPR = zeros(1,Nframe);
for index = 1:length(N)
Nbps = N(index);
M=2^Nbps; % Modulation order=2/4/6 for QPSK/16QAM/64QAM
for i = 1:length(SNR)
for j = 1:Nframe
Neb = 0;
X= (randi(M,1,Nfdma) - 1); % Row vector of the symbols to
be transmitted
Xmod= qammod(X,M,0,'gray')/norms(Nbps); % M-ary QAM
modulation
X_fdma = dst(Xmod,Nfdma);
X_ifdma(1:2:(2*Nfdma)) = X_fdma;
X_ifft = ifft(X_ifdma,Nfft);
if (i == 1)
sym_pow = X_ifft.*conj(X_ifft); % measure symbol power
PAPR(j) = max(sym_pow)/mean(sym_pow); % measure PAPR
end
X_GI = [X_ifft((Nfft - Nfft/4) + 1):Nfft) X_ifft];
y_GI = awgn(X_GI,SNR(i),'measured');
y = y_GI((Nfft/4)+1):(Nfft + Nfft/4));
Y = fft(y,Nfft);
Y_fdma = Y(1:2:(2*Nfdma));
Y_fdma = idst(Y_fdma,Nfdma);
X_r=qamdemod(Y_fdma*norms(Nbps),M,0,'gray');
Neb=Neb+sum(sum(de2bi(X_r,Nbps) ~= de2bi(X,Nbps)));
Berebn0(j) = Neb/(Nfft*Nbps);
end
Ber(index,i) = mean(Berebn0);
end
ccdf(index,:) = CCDF_calculation(PAPR,Nframe);
end
BER = Ber;
CCDF = ccdf;
end

%% This function simulates the IFDMA scheme for AWGN channel using DCT
function [BER,CCDF] = IFDMA_DCT(Nfft,Nfdma,N,SNR)
Nframe = 500;
Berebn0 = zeros(1,Nframe);
Ber = zeros(length(N),length(SNR));

```

```

norms=[1 sqrt(2) 0 sqrt(10) 0 sqrt(42)]; % BPSK 4-QAM/QPSK 16-QAM 64-
QAM
X_ifdma = zeros(1,Nfft);
PAPR = zeros(1,Nframe);
for index = 1:length(N)
    Nbps = N(index);
    M=2^Nbps; % Modulation order=2/4/6 for QPSK/16QAM/64QAM
    for i = 1:length(SNR)
        for j = 1:Nframe
            Neb = 0;
            X= (randi(M,1,Nfdma) - 1); % Row vector of the symbols to
be transmitted
            Xmod= qammod(X,M,0,'gray')/norms(Nbps); % M-ary QAM
modulation
            X_fdma = dct(Xmod,Nfdma);
            X_ifdma(1:(Nfft/Nfdma):end) = X_fdma;
            X_ifft = ifft(X_ifdma,Nfft);
            if (i == 1)
                sym_pow = X_ifft.*conj(X_ifft); % measure symbol power
                PAPR(j) = max(sym_pow)/mean(sym_pow); % measure PAPR
            end
            X_GI = [X_ifft((Nfft - Nfft/4) + 1):Nfft) X_ifft];
            y_GI = awgn(X_GI,SNR(i),'measured');
            y = y_GI((Nfft/4)+1):(Nfft + Nfft/4));
            Y = fft(y,Nfft);
            Y_fdma = Y(1:(Nfft/Nfdma):end);
            Y_fdma = idct(Y_fdma,Nfdma);
            X_r=qamdemod(Y_fdma*norms(Nbps),M,0,'gray');
            Neb=Neb+sum(sum(de2bi(X_r,Nbps) ~= de2bi(X,Nbps)));
            Berebn0(j) = Neb/(Nfft*Nbps);
        end
        Ber(index,i) = mean(Berebn0);
    end
    ccdf(index,:) = CCDF_calculation(PAPR,Nframe);
end
BER = Ber;
CCDF = ccdf;
end

```

```

%% This function simulates the IDFMA scheme for AWGN channel using DST
function [BER,CCDF] = IFDMADST(Nfft,Nfdma,N,SNR)
    Nframe = 500;
    Berebn0 = zeros(1,Nframe);
    Ber = zeros(length(N),length(SNR));
    norms=[1 sqrt(2) 0 sqrt(10) 0 sqrt(42)]; % BPSK 4-QAM/QPSK 16-QAM 64-
QAM
    PAPR = zeros(1,Nframe);
    X_ifdma = zeros(1,Nfft);
    for index = 1:length(N)
        Nbps = N(index);
        M=2^Nbps; % Modulation order=2/4/6 for QPSK/16QAM/64QAM
        for i = 1:length(SNR)
            for j = 1:Nframe
                Neb = 0;

```

```

X= (randi(M,1,Nfdma) - 1); % Row vector of the symbols to
be transmitted
Xmod= qammod(X,M,0,'gray')/norms(Nbps); % M-ary QAM
modulation
X_fdma = dst(Xmod,Nfdma);
X_ifdma(1:(Nfft/Nfdma):end) = X_fdma;
X_ifft = ifft(X_ifdma,Nfft);
if (i == 1)
    sym_pow = X_ifft.*conj(X_ifft); % measure symbol power
    PAPR(j) = max(sym_pow)/mean(sym_pow); % measure PAPR
end
X_GI = [X_ifft((Nfft - Nfft/4) + 1):Nfft) X_ifft];
y_GI = awgn(X_GI,SNR(i),'measured');
y = y_GI((Nfft/4)+1):(Nfft + Nfft/4));
Y = fft(y,Nfft);
Y_fdma = Y(1:(Nfft/Nfdma):end);
Y_fdma = idst(Y_fdma,Nfdma);
X_r=qamdemod(Y_fdma*norms(Nbps),M,0,'gray');
Neb=Neb+sum(sum(de2bi(X_r,Nbps) ~= de2bi(X,Nbps)));
Berebn0(j) = Neb/(Nfft*Nbps);
end
Ber(index,i) = mean(Berebn0);
end
ccdf(index,:) = CCDF_calculation(PAPR,Nframe);
end
BER = Ber;
CCDF = ccdf;
end

```

```

%% This function simulates the LDFMA scheme for AWGN channel using DCT
function [BER,CCDF] = LDFMADCT(Nfft,Nfdma,N,SNR)
Nframe = 500;
Berebn0 = zeros(1,Nframe);
Ber = zeros(length(N),length(SNR));
norms=[1 sqrt(2) 0 sqrt(10) 0 sqrt(42)]; % BPSK 4-QAM/QPSK 16-QAM 64-
QAM
PAPR = zeros(1,Nframe);
for index = 1:length(N)
    Nbps = N(index);
    M=2^Nbps; % Modulation order=2/4/6 for QPSK/16QAM/64QAM
    for i = 1:length(SNR)
        for j = 1:Nframe
            Neb = 0;
            X= (randi(M,1,Nfdma) - 1); % Row vector of the symbols to
be transmitted
            Xmod= qammod(X,M,0,'gray')/norms(Nbps); % M-ary QAM
modulation
            X_fdma = [dct(Xmod,Nfdma) zeros(1,Nfft-Nfdma)];
            X_ifft = ifft(X_fdma,Nfft);
            if (i == 1)
                sym_pow = X_ifft.*conj(X_ifft); % measure symbol power
                PAPR(j) = max(sym_pow)/mean(sym_pow); % measure PAPR
            end
            X_GI = [X_ifft((Nfft - Nfft/4) + 1):Nfft) X_ifft];
            y_GI = awgn(X_GI,SNR(i),'measured');
            y = y_GI((Nfft/4)+1):(Nfft + Nfft/4));
            Y = fft(y,Nfft);

```

```

        Y_fdma = Y(1:Nfdma);
        Y_fdma = idct(Y_fdma,Nfdma);
        X_r=qamdemod(Y_fdma*norms(Nbps),M,0,'gray');
        Neb=Neb+sum(sum(de2bi(X_r,Nbps) ~= de2bi(X,Nbps)));
        Berebn0(j) = Neb/(Nfft*Nbps);
    end
    Ber(index,i) = mean(Berebn0);
end
ccdf(index,:) = CCDF_calculation(PAPR,Nframe);
end
BER = Ber;
CCDF = ccdf;
end

%% This function simulates the LFDMA scheme for AWGN channel using DST
function [BER,CCDF]= LFDMA_DST(Nfft,Nfdma,N,SNR)
    Nframe = 500;
    Berebn0 = zeros(1,Nframe);
    Ber = zeros(length(N),length(SNR));
    norms=[1 sqrt(2) 0 sqrt(10) 0 sqrt(42)]; % BPSK 4-QAM/QPSK 16-QAM 64-
    QAM
    PAPR = zeros(1,Nframe);
    for index = 1:length(N)
        Nbps = N(index);
        M=2^Nbps; % Modulation order=2/4/6 for QPSK/16QAM/64QAM
        for i = 1:length(SNR)
            for j = 1:Nframe
                Neb = 0;
                X= (randi(M,1,Nfdma) - 1); % Row vector of the symbols to
                be transmitted
                Xmod= qammod(X,M,0,'gray')/norms(Nbps); % M-ary QAM
                modulation
                X_fdma = [dst(Xmod,Nfdma) zeros(1,Nfft-Nfdma)];
                X_ifft = ifft(X_fdma,Nfft);
                if (i == 1)
                    sym_pow = X_ifft.*conj(X_ifft); % measure symbol power
                    PAPR(j) = max(sym_pow)/mean(sym_pow); % measure PAPR
                end
                X_GI = [X_ifft((Nfft - Nfft/4) + 1):Nfft) X_ifft];
                y_GI = awgn(X_GI,SNR(i),'measured');
                y = y_GI((Nfft/4)+1):(Nfft + Nfft/4));
                Y = fft(y,Nfft);
                Y_fdma = Y(1:Nfdma);
                Y_fdma = idst(Y_fdma,Nfdma);
                X_r=qamdemod(Y_fdma*norms(Nbps),M,0,'gray');
                Neb=Neb+sum(sum(de2bi(X_r,Nbps) ~= de2bi(X,Nbps)));
                Berebn0(j) = Neb/(Nfft*Nbps);
            end
            Ber(index,i) = mean(Berebn0);
        end
        ccdf(index,:) = CCDF_calculation(PAPR,Nframe);
    end
    BER = Ber;
    CCDF = ccdf;
end

```

REFERENCES

- [1] R.W. Chang, "Synthesis of Band-Limited Orthogonal Signals for Multichannel Data Transmission", *Bell Syst. Tech. J.*, vol.45, pp. 1775-1796, Dec. 1966.
- [2] B.R. Salzberg, "Performance of an efficient parallel data transmission system", *IEEE Trans. Communication Technol.*, vol. COM-15, pp. 805-813, Dec. 1967.
- [3] S.B. Weinstein and P.M. Ebert, "Data transmission by frequency-division multiplexing using the discrete Fourier transform", *IEEE Trans. Communication Technol.*, vol. COM-19, pp. 628-634, Oct. 1971
- [4] John G.Proakis, Dimitris G.Manolakis, Digital signal processing, Principles, Algorithms, and Applications, Prentice- Hall publications
- [5] R. Van Nee and R. Prasad, "OFDM for Wireless Multimedia Applications", Artech House Publishers, 2000
- [6] Eldo Mabiala, Mathias Coinchon , Karim Maouche "Study of OFDM modulation" Eurecom institute, December 1999
- [7] B. Muquet, Z. Wang, G. Giannakis, M. de Courville, and P. Duhamel, "Cyclic prefixing or zero padding for wireless multicarrier transmissions," *IEEE Trans. Commun.*, vol. 50, no. 12, pp. 2136–2148,
- [8] M. Huemer, C. Hofbauer, A. Onic, and J. B. Huber, "Design and analysis of UW OFDM signals," *{AEU} - International Journal of Electronics and Communications*, vol. 68, no. 10, pp. 958–968, 2014
- [9] C. Hofbauer and M. Huemer, "A study of data rate equivalent UW OFDM and CP OFDM concepts", *Forty Sixth Asilomar Conference on Signals, Systems and Computers (ASILOMAR 2012)*, pp. 173–177,
- [10] H. Steendam, "Theoretical performance evaluation and optimization of UW OFDM", *IEEE Transactions on Communications*, vol. 64, no. 4, pp. 1739–1750, 2016.
- [11] G. Berardinelli et al., "Zero-Tail DFT-Spread-OFDM Signals," *Proc. IEEE GLOBECOM Wksp.*, Dec. 2013, pp. 229–34.
- [12] G. Berardinelli et al., "On the Potential of Zero-Tail DFT-Spread-OFDM as 5G Waveform," *Proc. IEEE VTC-Fall*, Sept. 2014, pp. 1–5.
- [13] J. Abdoli, M. Jia, and J. Ma, "Filtered OFDM: A new waveform for future wireless systems," in *Proc. IEEE 16th Int. Workshop Signal Process. Adv. Wireless Commun. (SPAWC), Stockholm, Sweden*, Jun./Jul. 2015, pp. 66–70.
- [14] G. Fettweis, M. Krondorf, and S. Bittner, "GFDM—Generalized frequency division multiplexing," in *Proc. IEEE 69th Veh. Technol. Conf. (VTC)*, Barcelona, Spain, Apr. 2009, pp. 1–4
- [15] Y. Kus, M. Kavlak, U. Elmagöz and A. Özen, "A Novel Waveform Design Based on Discrete Sine Transform for 5G and beyond," *2018 41st International Conference on Telecommunications and Signal Processing(TSP)*, Athens,2018,pp. 1-4
- [16] F. Daffara, and O.Adami, " A new frequency detector for orthogonal multi-carrier transmission techniques," *IEEE VTC*,1995, pp. 804-809

- [17] Moose, P.H. (1994) A technique for orthogonal frequency division multiplexing frequency offset correction," *IEEE Trans. Commun.*, 42, 2908-2914
- [18] F. Classen and H. Myer, " Frequency synchronization algorithm for OFDM systems suitable for communication over frequency selective fading channels," *IEEE VTC'94*, pp. 1655–1659.
- [19] van Nee, R. and de Wild, A. (May 1998) Reducing the peak-to-average power ratio of OFDM," *IEEE VTC'98*, vol.3, pp. 18-21
- [20] Li, X. and Cimini, L.J. (1998) Effects of clipping and filtering on the performance of OFDM," *IEEE Commun. Letter*, 2(20), 131-133
- [21] Wilkinson, T.A. and Jones, A.E. (July 1995) Minimization of the peak-to-mean envelope power ratio of multicarrier transmission scheme by block coding," *IEEE VTC'95*, Chicago, vol. 2, pp. 825–829.
- [22] Davis, J.A. and Jedwab, J. (1999) Peak-to-mean power control in OFDM, Golay complementary sequences, and Reed-Mueller codes," *IEEE Trans. Info. Theory*, 45(7), 2397–2417.
- [23] Park, M.H. et al. (2000) PAPR reduction in OFDM transmission using Hadamard transform," *IEEE ICC'00*, vol. 1, pp. 430-433
- [24] Galda, D. and Rohling, H. (2002) A low complexity transmitter structure for OFDM-FDMA uplink systems," *IEEE VTC*, 2002, vol 4. Pp. 1737-1741
- [25] Myung, H.G., Lim, J., and Goodman, D.J. (2006) Single carrier FDMA for uplink wireless transmission," *IEEE Vehicular Magazine*, 1(3), 30-38
- [26] Myung, H.G., Lim, J., and Goodman, D.J. (Sept. 2006) Peak-to-average power ratio of single carrier FDMA signals with pulse shaping," *PIMRC*, 2006, pp. 1-5
- [27] N. Ahmed, T. Natarajan and K.R. Rao, "Discrete Cosine Transform," *IEEE trans. Computers*, vol. C-23, pp. 90-93, Jan. 1974
- [28] Jain A.K. "A fast Karhunen-Loeve Transform for a class of random processes," *IEEE trans. Commun.*, vol. Com-24, September 1023-1029 (1976).
- [29] S. Dhamija, P. Jain, "Comparative Analysis for Discrete Sine Transform as suitable method for noise estimation," *IJCSI*, 2018, pp. 162-164